

UNIVERSITY OF CALIFORNIA, MERCED

**A Mass Balance Model of Lyell and  
Maclure Glaciers in Yosemite National  
Park**

by

Kevin Anthony Mendoza

A thesis submitted in fulfillment for the  
degree of Bachelors of Science

in the  
Applied Photonics Research Group  
Jay E. Sharping  
School of Natural Sciences

April 2015

# Declaration of Authorship

I, Kevin Anthony Mendoza, declare that this thesis titled, ‘A Mass Balance Model of Lyell and Maclure Glaciers in Yosemite National Park’ and the work presented in it are my own. I confirm that:

- This work was done wholly or mainly while in candidature for a research degree at this University.
- Where any part of this thesis has previously been submitted for a degree or any other qualification at this University or any other institution, this has been clearly stated.
- Where I have consulted the published work of others, this is always clearly attributed.
- Where I have quoted from the work of others, the source is always given. With the exception of such quotations, this thesis is entirely my own work.
- I have acknowledged all main sources of help.
- Where the thesis is based on work done by myself jointly with others, I have made clear exactly what was done by others and what I have contributed myself.

Signed:

---

Date:

---

*“It is not the mountain we conquer, but ourselves.”*

Sir Edmund Hillary

## *Abstract*

Jay E. Sharping

School of Natural Sciences

Bachelors of Science

by Kevin Anthony Mendoza

The Lyell and Maclure Glaciers, two historically important glaciers of Yosemite National Park, have been rapidly retreating since their discovery in 1872. The only two water balance studies done on these glaciers were conducted on the Maclure Glacier during the 1967-1974 hydrologic years [Tangborn, 1977, Dean, 1974]. Here I attempt to quantify the water balance of two basins containing these glaciers. Water inputs were calculated by applying snow pillow data from the California Department of Water Resources/Snow Surveys and two precipitation vs. elevation slope models from Rice [2011]. Water outputs consisted of a simplified evapotranspiration model derived from Lundquist [2011], and water runoff data from the National Park Service [National Park Service, Unpublished Hydrologic Data]. 56 Linear combinations of precipitation and evaporation models were used to develop water balance models. It was found that most of these models predicted melt rates from these two glaciers outside empirical observations recorded by the National Park Service. However both Lyell Glacier Basin and the Lyell Fork of the Tuolumne Basin water balance spreads had statistically notable Kolmogorov-Smirnov test statistics: Lyell Glacier with  $p = 0.34$  for 2013 and  $p = 0.37$  for 2014, and Lyell Fork with  $p = 0.45$  for 2009. The basin containing Lyell Glacier had a water balance spread of between  $-1,105 \times 10^3 m^3$  and  $+58 \times 10^3 m^3$  (interquartile range) with a mean of  $-564 \times 10^3 m^3$  for the 2013 hydrologic year, and between  $-1,137 \times 10^3 m^3$  and  $+21 \times 10^3 m^3$  (interquartile range) with a mean of  $-583 \times 10^3 m^3$  for the 2014 hydrologic year. The Lyell fork of the Tuolumne basin containing both Lyell and Maclure Glaciers had a water balance spread of between  $-14,350 \times 10^3 m^3$  and  $+7,454 \times 10^3 m^3$  (interquartile range) with a mean of  $-2,426 \times 10^3 m^3$  for the 2009 hydrologic year. Based on Tangborn [1977], Dean [1974], and Basagic and Fountain [2011], the variations observed in water balance models for Lyell Glacier in this study are an order of magnitude larger than the expected melt signal, and two orders of magnitude for the Lyell Fork of the Tuolumne water balance models. This lack of precision is likely from the precipitation and evapotranspiration models used.

## *Acknowledgements*

The author would like to thank the many contributors to this study from the National Park Service: Dr. Greg Stock, Harrison Forrester, Jim Roche, Lyman Petersen, Laura Walkup, and Perri Sasnett. Laura Walkup was responsible for providing discharge data for the Tuolumne FATB basin. Perri Sasnett conducted crucial hypsometry and basin cover analysis that provided the basis for the evapotranspiration estimates. Dr. Greg Stock in particular provided valuable direction and feedback throughout the entire course of this study.

Several persons from the University of California, Merced also provided valuable feedback and encouragement: Dr. Carrie Menke, Dr. Marylin Fogel, Dr. Roger Bales, Dr. Michael Scheibner, Joy Baccei, Dr. Mohammad Safeeq, and Dr. Jay Sharping. Dr. Sharping in particular took a large leap of faith in letting the author propose, devise, and ultimately execute a custom thesis project.

Dr. Robert Anderson from the University of Colorado, Boulder also deserves credit for assisting Dr. Stock with several numerical models and laying the initial framework that made this study possible.

Adi Lopez received her first art commission through this project; her unique style of water color painting contributed to this project greatly.

Jessica Chang should be noted as chief editor of this thesis, because the author's young undergraduate self is still getting his feet wet with writing in the sciences.

Most importantly Ken Watson, Jesse Chakrin, Maynard Medefind, Dan Martinez, Andres Estrada, and Aricia Martinez made my professional relationship to Yosemite's RMS division possible through their efforts to help me follow my passion inside the National Park Service.

# Contents

<b>Declaration of Authorship</b>	<b>i</b>
<b>Abstract</b>	<b>iii</b>
<b>Acknowledgements</b>	<b>iv</b>
<b>List of Figures</b>	<b>viii</b>
<b>List of Tables</b>	<b>ix</b>
<b>Abbreviations</b>	<b>x</b>
<b>Symbols</b>	<b>xi</b>
<b>1 Introduction</b>	<b>1</b>
1.1 Previous Studies . . . . .	2
1.2 Motivation for Further Study . . . . .	4
<b>2 Study Design</b>	<b>6</b>
2.1 Water Balance Modelling . . . . .	6
2.1.1 Characterization of Relevant Variables . . . . .	7
2.1.2 Evaporative Terms . . . . .	8
2.1.3 Groundwater Flux . . . . .	9
2.1.4 Ablation . . . . .	9
2.1.5 Glacial Loss . . . . .	9
2.1.6 Precipitation . . . . .	10
2.1.7 Runoff . . . . .	11
2.1.8 The Basin Water Balance Equation . . . . .	12
2.2 Available Instruments and Data . . . . .	12
2.2.1 Meteorologic stations . . . . .	13
2.2.2 Solinst Levelogger Gold . . . . .	14
2.2.3 Upper and Lower Twin Bridges Discharge Datasets . . . . .	14
2.2.4 Park Cover Map . . . . .	15
2.3 Study Area Characterization . . . . .	16
2.3.1 The Lyell Fork of the Tuolumne River . . . . .	17

2.3.2	Maclure Creek	18
2.3.3	Lyell Creek Below Confluence	18
2.3.4	Lyell Creek Above Confluence	19
2.3.5	Rafferty Creek	19
2.4	Possible Complications	19
2.4.1	Cold Temperatures	19
2.4.2	Timing of Spring Pulse	20
<b>3</b>	<b>Data Analysis</b>	<b>21</b>
3.1	Logger Complications	21
3.1.1	Suspicious Data	21
3.1.1.1	Expected Data Trends	21
3.1.1.2	Rafferty Creek Logger	22
3.1.1.3	Maclure Creek Logger	23
3.1.1.4	Lyell Creek	25
3.1.2	Potential Physical Explanations	26
3.1.2.1	Freezing Experiment	28
3.1.3	Logger Methodology Conclusions	29
3.2	Discharge Dataset	30
3.2.1	Monsoonal Event Correction	31
3.2.2	Maclure and Lyell Discrepancies	32
3.2.3	Twin Bridges Discharge Dataset	32
3.3	Precipitation Data	33
3.3.1	Precipitation Models	33
3.3.2	Comparison With Discharge Data and Evapotranspiration	36
3.3.3	Precipitation Model Conclusion	37
3.4	Basin Balance Analysis	39
3.4.1	Lyell Creek Below Confluence Basin Balance Results	40
3.4.1.1	All Balance Models	40
3.4.1.2	Conforming Balance Models	40
3.4.2	Maclure Creek Basin Balance Results	41
3.4.2.1	All Balance Models	41
3.4.2.2	Conforming Balance Models	41
3.4.3	Lyell Creek Above Confluence Balance Results	42
3.4.3.1	All Balance Models	42
3.4.3.2	Conforming Balance Models	43
3.4.4	Tuolumne Fork Above Twin Bridges Basin Balance	44
3.4.4.1	All Balance Models	44
3.4.4.2	Conforming Balance Models	45
<b>4</b>	<b>Conclusion</b>	<b>55</b>
4.1	Water Balance at Tuolumne River Above Twin Bridges	55
4.2	Water Balance at Lyell Creek Above Confluence with Maclure Creek	56
4.3	Comparison With Similar Studies	57
4.4	Suggestions For Future Studies	58



# List of Figures

1.1	Lyell and Maclure Glaciers September 2014 . . . . .	2
1.2	Lyell Glacier in 1941 vs 2012 . . . . .	4
2.1	Artistic Rendition of Basin Fluxes . . . . .	7
2.2	Study site within Yosemite National Park . . . . .	16
2.3	Study Basins and Important Locations . . . . .	17
3.1	Rafferty Creek Logger Data . . . . .	22
3.2	Maclure Creek Logger Data . . . . .	24
3.3	Lyell Creek Above Confluence Logger Data . . . . .	25
3.4	The Expanding Ice Hypothesis . . . . .	26
3.5	The Ice Pipe Hypothesis . . . . .	27
3.6	The Negative Pressure Hypothesis . . . . .	28
3.7	Matlab Negative Pressure Simulation . . . . .	29
3.8	The Freezing Experiment . . . . .	30
3.9	Lyell Creek BLWC and Maclure Creek Discharge Data . . . . .	31
3.10	Discharge Series for Tuolumne Fork Above Twin Bridges . . . . .	33
3.11	Snow Water Equivalent Elevation Trends . . . . .	34
3.12	Lyell BLWC and Maclure Basin Precipitation Models. . . . .	35
3.13	Precipitation Models for the Lyell Fork of the Tuolumne at Twin Bridges Site . . . . .	36
3.14	Tuolumne FATB Precipitation Models and Cumulative Discharge . . . . .	37
3.15	Lyell BLWC and Maclure Creek Basin Cumulative Discharge and Precipitation . . . . .	38
3.16	Lyell Creek BLWC Basin Water Balance . . . . .	46
3.17	Lyell Creek Basin BLWC Glacial Melt Constants . . . . .	46
3.18	Maclure Creek Basin Water Balance . . . . .	47
3.19	Maclure Creek Basin Glacial Melt Constants . . . . .	47
3.20	Lyell Creek ABVC Basin Water Balance . . . . .	48
3.21	Lyell Creek ABVC Basin Glacial Melt Constants . . . . .	48
3.22	Tuolumne Fork Above Twin Bridges Basin Water Balance . . . . .	49
3.23	Tuolumne Fork Above Twin Bridges Basin Glacial Melt Constants . . . . .	50

# List of Tables

2.1	Flux Variable Summary . . . . .	7
2.2	Basin Percent Cover Type . . . . .	18
2.3	Basin Area by Percent Cover Type . . . . .	18
3.1	Average Snow Water Equivalent depth Estimates by Elevation for the Tuolumne River . . . . .	34
3.2	Expected Melt Signal Amplitude by Basin . . . . .	39
3.3	Calculated Basin Water Balance for Lyell Creek BLWC Basin . . . . .	51
3.4	Calculated Glacial Melt Constants for Lyell Creek BLWC Basin . . . . .	51
3.5	Calculated Basin Water Balance for Maclure Creek Basin . . . . .	51
3.6	Calculated Glacial Melt Constants for Maclure Creek Basin . . . . .	52
3.7	Calculated Basin Water Balance for Lyell Creek ABVC Basin . . . . .	52
3.8	Calculated Glacial Melt Constants for Lyell Creek ABVC Basin . . . . .	52
3.9	Calculated Basin Water Balance for Tuolumne Basin Above Twin Bridges	53
3.10	Calculated Glacial Melt Constants for Tuolumne Basin Above Twin Bridges	53
3.11	Selected Basin and Year Water Balance Quantile Statistics . . . . .	54
3.12	Basin and Year Glacial Melt Constant Quantile Statistics . . . . .	54

# Abbreviations

<b>ACC</b>	<b>A</b> nthropogenic <b>C</b> limate <b>C</b> hange
<b>MBM</b>	<b>M</b> ass <b>B</b> alance <b>M</b> odel
<b>NPS</b>	<b>N</b> ational <b>P</b> ark <b>S</b> ervice
<b>RMS</b>	<b>R</b> esource <b>M</b> anagement & <b>S</b> cience <b>D</b> ivision
<b>SWE</b>	<b>S</b> now <b>W</b> ater <b>E</b> quivalent
<b>USGS</b>	<b>U</b> nited <b>S</b> tates <b>G</b> eological <b>S</b> urvey
<b>YNP</b>	<b>Y</b> osemite <b>N</b> ational <b>P</b> ark
<b>BLWC</b>	<b>B</b> elow <b>C</b> onfluence
<b>ABVC</b>	<b>A</b> bove <b>C</b> onfluence
<b>FATB</b>	<b>F</b> ork <b>A</b> bove <b>T</b> win <b>B</b> ridges
<b>MET</b>	<b>M</b> eteorologic
<b>KT</b>	<b>K</b> olmogorov- <b>S</b> mirnov
<b>IQR</b>	<b>I</b> nter <b>Q</b> uartile <b>R</b> ange

# Symbols

Symbol	Name	Unit
$Q$	Cumulative Runoff	$\text{m}^3/\text{m}^2$ water
$P$	Precipitation	$\text{m}^3/\text{m}^2$ water
$E_T$	Evapotranspiration	$\text{m}^3/\text{m}^2$ water
$E_S$	Evapotranspiration	$\text{m}^3/\text{m}^2$ water
$E_0$	Evapotranspiration	$\text{m}^3/\text{m}^2$ water
$E$	All Evaporative Losses	$\text{m}^3/\text{m}^2$ water
$\Delta G$	All Evaporative Losses	$\text{m}^3/\text{m}^2$ water
$\Delta M$	Glacier Melt Contribution	$\text{m}^3/\text{m}^2$ water
$\Delta B$	Ablation/Avalanching flux	$\text{m}^3/\text{m}^2$ water
$T$	Mean Summer Temperature	$^{\circ}\text{C}$
$A$	Area	$\text{m}^2$
$a_i$	Fractional Ice Area	unitless
$a_e$	Fractional Evaporative Loss Area	unitless
$g$	Basin Glacial Melt Contribution Parameter	$\text{m}^3/\text{m}^2$ water $^{\circ}\text{C}^{-1}$
$g_0$	Ice Area-Adjusted Glacial Melt Contribution Parameter	$\text{m}^3/\text{m}^2$ water $^{\circ}\text{C}^{-1}$
$e$	Evaporative Constant	$\text{m}^3/\text{m}^2$ water
$q(t)$	Discharge	$\text{m}^3 \text{s}^{-1}$ water
$Y(t)$	Stage	m water
$t$	Time	s
$u$	Stream Velocity	$\text{m s}^{-1}$
$a$	Stream Cross Sectional Area	$\text{m}^2$
$S$	Local Slope Gradient	$\text{m m}^{-1}$
$c$	Discharge Constant	$\text{m}^6 \text{m}^{-5} \text{s}^{-1}$
$C_T$	Temperature-based Glacial Melt Constant	m SWE/ $^{\circ}\text{C}$

---

$C_P$	Precipitation-based Glacial Melt Constant	m SWE / m Precipitation
$\alpha$	Empirical Logger Offset	m water

*Dedicated to my grandparents Joe and Emma Sanchez. The dedication they've given to family will bear fruits far beyond what they know. ...*

# Chapter 1

## Introduction

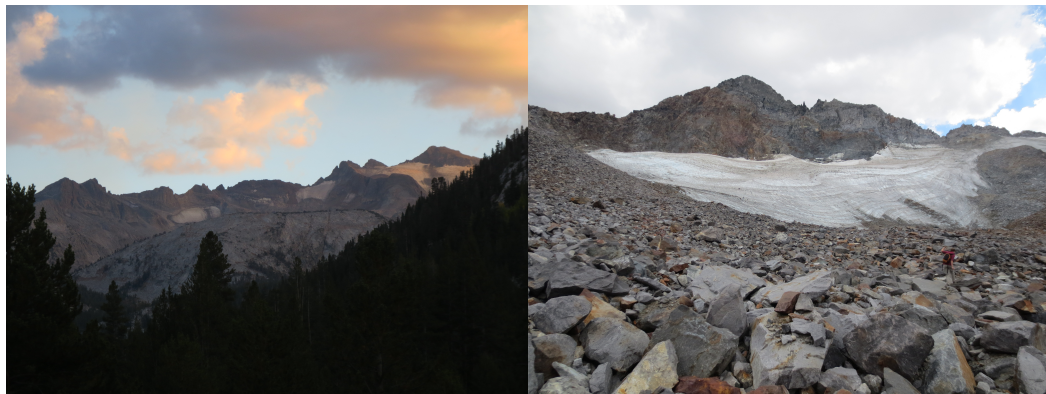
*"The Lyell Glacier is about a mile wide and less than a mile long, but presents, nevertheless, all the essential characters of large, river-like glaciers.. it is all the more interesting since it is the highest and most enduring remnant of the great Tuolumne Glacier, whose traces are still distinct fifty miles away, and whose influence on the landscape was so profound.*

-John Muir, The Yosemite.

Nestled high up in the crest of the Sierra Nevada, the Lyell and Maclure Glaciers have attracted backpackers and researchers alike for over a hundred years. The beautiful and ecologically diverse Tuolumne Meadows are watered year round by the melting ice, and many highly trafficked campgrounds within Yosemite National Park depend upon this runoff late season as their sole water supply. Recently, several studies have observed dramatic losses in these two ice bodies. Climate models forecast increased average temperatures and decreases in winter precipitation across the region. Although extensive transect and repeat photography surveys on these two glaciers have been done, only two studies ever attempted to quantify the rate of melt of these glaciers.

In this thesis, we set out to quantify the water balance of Lyell and Maclure Glaciers. Repeat photography, perimeter and, and elevation transect surveys conducted in the last thirty years confirm both glaciers are in rapid retreat. While these surveys can quantify some aspects of glacial retreat, only through use of a water balance model can accurate calculations of water volume loss be made. Additionally previous studies have focused on the glaciers as an isolated system; this study seeks to discover what the impact of reductions in base flow will have on the basin hydrology. Several pressure loggers were deployed around the glaciers in an attempt to measure glacial runoff. Evapotranspiration models were estimated based on observed minimums and maximums from a study done

in an alpine basin to the south. Precipitation inputs were based on maximum winter snow water equivalent. It was found that most models were unreliable, having balance distributions similar to that of a uniform distribution. Three of these had Kolmogorov-Smirnov test statistics worth mentioning: Lyell Glacier with  $p = 0.34$  for 2013 and  $p = 0.37$  for 2014, and Lyell Fork with  $p = 0.45$  for 2009. The basin containing Lyell Glacier had a water balance spread of between  $-1,105 \times 10^3 m^3$  and  $+58 \times 10^3 m^3$  (interquartile range) with a mean of  $-564 \times 10^3 m^3$  for the 2013 hydrologic year, and between  $-1,137 \times 10^3 m^3$  and  $+21 \times 10^3 m^3$  (interquartile range) with a mean of  $-583 \times 10^3 m^3$  for the 2014 hydrologic year. The Lyell Fork of the Tuolumne basin containing both Lyell and Maclure Glaciers had a water balance spread of between  $-14,350 \times 10^3 m^3$  and  $+7,454 \times 10^3 m^3$  (interquartile range) with a mean of  $-2,426 \times 10^3 m^3$  for the 2009 hydrologic year. Uncertainties in ice area and volume of melt during the study years make it hard to compare these data to expected melt signal. However, a first order guess suggests that all three of these water balances interquartile ranges are at least an order of magnitude larger than the expected glacial melt signal. Future studies should focus on improving precipitation and evapotranspiration models, as these were the major limitations of this study. These improvements should be done as soon as possible as the rapid melting of these two glaciers provides little time for more research.



(A) Lyell Glacier East and West Lobes

(B) Maclure Glacier

FIGURE 1.1: Lyell and Maclure Glaciers September 2014  
The Lyell and Maclure Glaciers as they appeared to the RMS research team  
September 2014. Photos taken by author.

## 1.1 Previous Studies

John Muir first identified englacial features within and turbid meltwater emanating from the Lyell Glacier and performed stake velocity measurements in the Maclure Glacier in 1872, where he found the average rate of movement to be 2.5 cm/day [Muir, 1871]. He also invited Dr. Joseph LeConte, then a Professor at the University of California,

---

Berkeley, to observe the glaciers in the Tuolumne Region, where he later corroborated Muir's findings [LeConte, 1900].

Russell [1885] drafted the first map of these glaciers in 1885, publishing his findings in the USGS's Annual Report. Gilbert [1905] undertook the first study of changes in Lyell Glacier, and although he concluded little changed between 1883 and 1903, a later study by Currey [1969] found that the glaciers had retreated and advanced back to their original 1883 positions by 1903.

The National Park Service began systematic surveys of the Lyell and Maclure Glaciers from 1931 to 1975 consisting of repeat photographs, perimeter surveys, and cross-glacial transects [National Park Service, 1931-1975]. They reported an increase in the area of the upper portions of both Maclure and Lyell Glaciers, with retreat and withdrawal of the lower portions. In 1970 they reported that portions of the Lyell Glacier were 15 meters lower than when transect surveys began. In 1975 NPS noted that there was more loss in the lower sections of both glaciers, but were not able to conduct further measurements due to funding issues.

Tangborn [1977] attempted to conduct a mass balance survey of the Maclure Glacier for the 1967 hydrologic year. A net gain of  $0.39\text{m} \pm 0.5\text{m}$  of vertical water column across the study basin and a loss of  $0.06\text{m} \pm 0.01\text{m}$  on the glacier itself was observed. However the research group noted that conditions at the study site may have affected the mass balance input terms, necessitating extrapolating mass balance input from adjusted measurements taken at a meteorologic station 26km away.

Dean [1974] performed a six year mass balance study of Maclure Glacier starting in 1967 and found that the glacier had a slight gain of 0.11m of water per year. It was noted that uncertainty in the winter mass balance was significant ( $\pm 20\%$  for winter balance,  $\pm 30\%$  for winter ablation of snow and ice)

Since 1974, no mass balance work has been done on either the Lyell or Maclure Glaciers, however repeat photography at several photo points by both the public and NPS surveys revealed little change in 1987 [Hardy, 1987].

Raub [2006] used areal photographic data from 1972 to develop a glacier and perennial ice inventory. Basagic and Fountain [2011] attempted to quantify rates of glacial change in the Sierra Nevada by utilizing area-volume relationships. It found that Lyell east lobe lost -40% of its area, Lyell west lobe lost -78% of its area, and Maclure lost -48% of its area from 1903 to 2004.

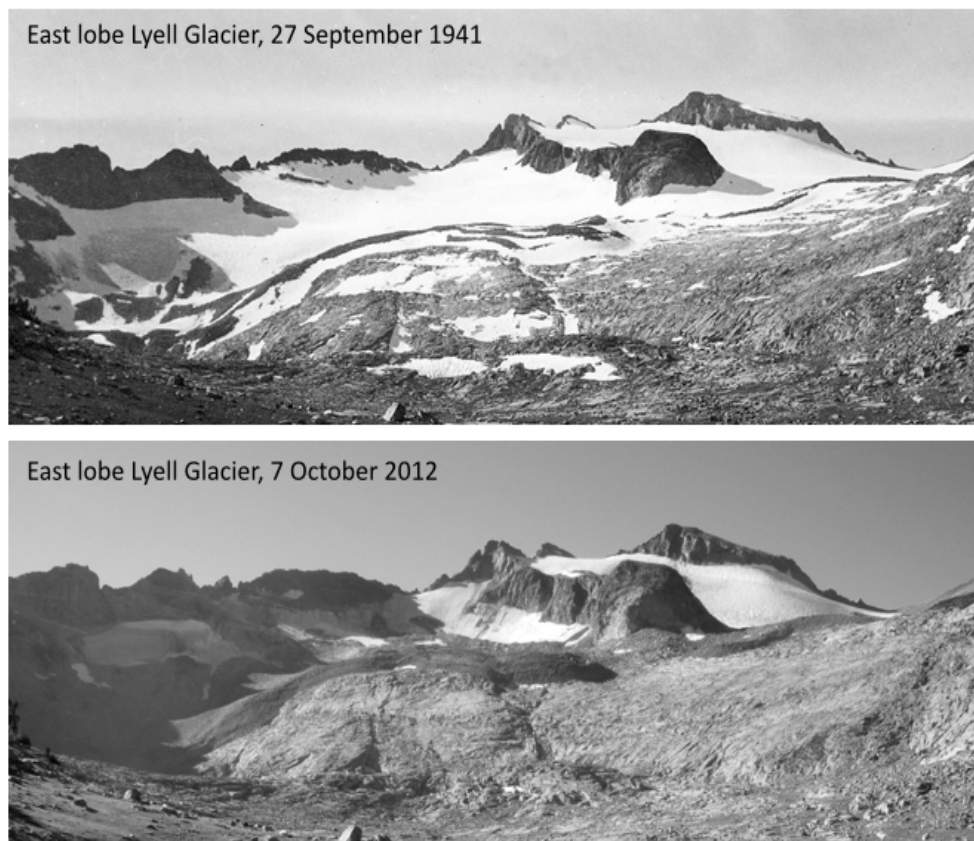


FIGURE 1.2: Lyell Glacier in 1941 vs 2012

Comparison Photo of Lyell Glacier in 1941 vs 2012. Both photos were taken by the National Park Service.

The [National Park Service, Unpublished Glacier Data](#) has resumed its efforts to survey these glaciers since 2002. Based on perimeter and elevation transect surveys, it is clear that these glaciers are undergoing extreme retreat.

## 1.2 Motivation for Further Study

Anthropogenic climate change has the potential to reduce the fraction of precipitation that falls as snow in this region [Kiparsky M, 2014, Lundquist, 2005]. Already Glacier National Park has observed its glaciers in retreat [Brown, 2010], and has estimated that under a  $+3^{\circ}\text{C}$  warming scenario, Sperry Glacier is likely to be completely gone by 2100. Arguably the Tuolumne River is more sensitive to climate change as it relies on only a few perennial bodies of ice to supply the basin with freshwater year round, yet only two mass balance studies have been conducted on the remaining glaciers in the drainage. Thus due to the potential effects of ACC on the glaciers themselves and the management

concerns the changing discharge from them creates, there is a need for a definitive mass balance model which quantifies the rate of water loss from these glaciers and examines the hydrologic nature of the basin post ice.

## Chapter 2

# Study Design

### 2.1 Water Balance Modelling

Glaciers respond to changes in weather patterns by advancing/growing forward during high precipitation years, and retreating/melting backwards during low precipitation years. Temperature also plays a role, with warm temperatures leading to increased melt vs. low temperatures. More generally the behavior of any glacier system is governed by a coupling between both net energy fluxes and net mass/water fluxes. Maclure and Lyell Glaciers present a challenge in that many of the variables needed develop an energy-mass balance model cannot be directly measured on the glacier. Because of this, and because of the remoteness of the site, it was determined that a water balance model was most appropriate for this study.

Water balance models (Also known as mass balance models) work by combining inter-system fluxes to calculate the net loss of water within the study area. Although they can be used to examine ice and water fluxes within different regions of the same glacier, the remoteness of these glaciers necessitates an expansion of the water balance method to basin scales. This is known as a hydrologic mass balance method and is outlined in [Paterson and Cuffey \[2010b\]](#). Many of the nuances of glacier retreat and advance cannot be derived by examining fluxes at this scale, but by quantifying the amount of water being lost or gained in the basin, predictions can be made as to the general behaviours of these glaciers.

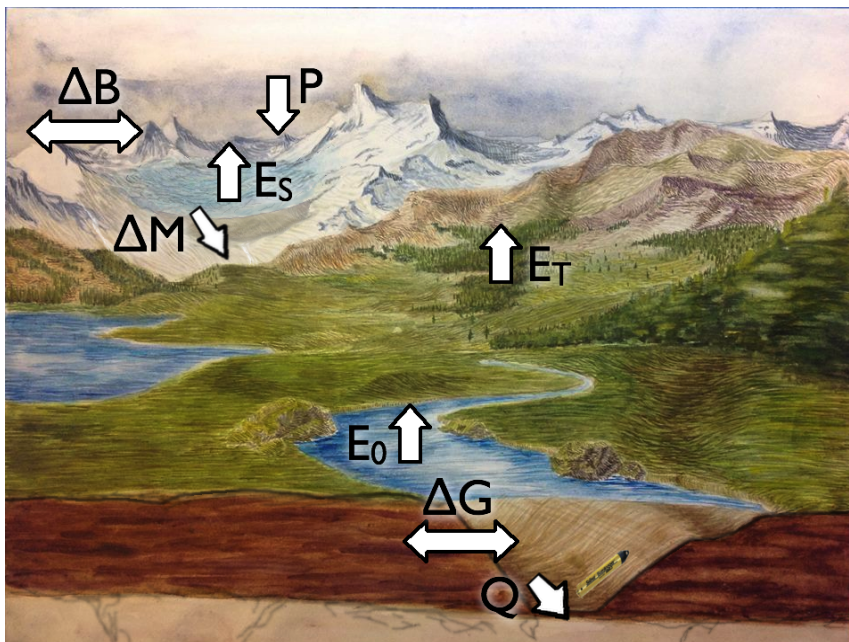


FIGURE 2.1: Artistic Rendition of Basin Fluxes

Illustrated here is an artistic rendition of major basin fluxes contained in table 2.1. Note that meadows also contribute to  $E_T$ , evapotranspiration. Watercolor painted by Lopez [2015].

Flux	Flux Type	Symbol
Surface Runoff	External	$Q$
Precipitation	External	$P$
Evaporation	External	$E_0$
Evapotranspiration	External	$E_T$
Sublimation	External	$E_S$
Groundwater Flux	Internal & External	$\Delta G$
Glacier-derived water Flux	Internal	$\Delta M$
Ablation/Accumulation Flux	External	$\Delta B$

TABLE 2.1: Flux Variable Summary

Summary of flux variables used in basin water balance models. Each is either a flux between the system and the external climate, or fluxes from internal water sources.

### 2.1.1 Characterization of Relevant Variables

All water entering the mass balance system can be classified as an external flux or an internal flux arising from a change in stored water. Accurate measurements of external fluxes can provide information on the depletion rate of inter-system pools, such as perennial ice bodies.

$$P + \Delta G + \Delta M + \Delta B = Q + E_0 + E_T + E_S \quad (2.1)$$

Variables outlined in table 2.1, equation 2.1, and illustrated in figure 2.1 comprise the major components of any hydrologic basin system containing perennial ice cover. Each variable has been normalized to represent vertical meters of water averaged over the relevant basin. Of these, only surface runoff  $Q$  can be accurately measured by instrumentation; all other variables must either be estimated or neglected due to basin characteristics.

### 2.1.2 Evaporative Terms

Evaporation  $E_0$ , evapotranspiration  $E_T$ , and sublimation  $E_s$  can be major factors in basin water balances [Kattelmann, 1991]. Numerous methods exist to empirically calculate each term [Fisher, 2005], but as a first order approximation they will be combined into a single variable,  $E$ . This simplifies equation 2.1 into 2.2.

$$P + \Delta G + \Delta M + \Delta B = Q + E \quad (2.2)$$

$E$  may depend on many environmental variables including daily mean temperature, snow cover, humidity, and albedo. Lundquist [2011] found in the Merced Basin adjacent to the study area that  $E$  varied in a high elevation (mean elevation 2750m) basin between 0.3 and 0.5 basin-averaged meters of water ( $Volume/Area$ , referred to as  $m^3/A$  for the rest of this paper). While this is a significant amount of water, the narrow envelope of values reported justifies estimating  $E$  as a constant. Furthermore if we assume that  $E$  is only dependent on the evaporative and transpirative surface area,  $E$  then obeys 2.3. Where  $a_e$  is the evaporative/transpirative area fraction and  $e$  is an evaporative constant in units of vertical meters of water per year.

$$E = a_e \cdot e \quad (2.3)$$

Rather than attempting to vary  $e$  to bring  $E$  to a mean value between  $0.3m^3/A$  and  $0.5m^3/A$  that is representative of the true evapotranspiration, two separate models will be examined: one where  $E$  is set to  $0.3m^3/A$  and one where  $E$  is set to  $0.5m^3/A$ . This assumption is likely to fail in the bare rock dominated upper basins within the study area, and instead the  $e$  values from the lower basins will be used to calculate ET based on the forest, open water, and meadow fraction.

### 2.1.3 Groundwater Flux

The study area is underlain by minimally fractured, largely unweathered mesozoic granite and metamorphic rocks. [Dingman \[2002\]](#) lists the hydraulic conductivity of unfractured igneous rocks as three orders of magnitude lower than hard sandstone, making it likely that groundwater contributions to the hydrologic balance are minimal. However, numerous meadows occupying sediment-filled depressions do exist both in the high elevation basins and lower elevation basins. While the sediment depth is assumed to be shallow due to numerous outcroppings of bedrock, these meadows may act as a small water source or sink. The long period of study is assumed to average any contributions from groundwater or meadow storage to zero.

### 2.1.4 Ablation

Ablation or accumulation due to wind blown snow  $\Delta B$  will be assumed to be zero, due to the sizes of the basins and the lack of any reasonable methodology to quantify the term.

### 2.1.5 Glacial Loss

As the main objective of this study is to determine the rate of mass loss from Lyell and Maclure Glaciers, the water flux from the melting glacier  $\Delta M$ , is the main variable of interest. According to [Paterson and Cuffey \[2010a\]](#) the annual mass balance of a temperate mountain glacier can be linearly approximated by 2.4.

$$\Delta M = \frac{\partial M}{\partial T} \cdot \Delta T + \frac{\partial M}{\partial P} \cdot \Delta P \quad (2.4)$$

Where  $\Delta T$  is the change in mean temperature during the melt season and  $\Delta P$  is the change in precipitation inputs.  $\frac{\partial M}{\partial T}$  and  $\frac{\partial M}{\partial P}$  are known as the climate sensitivity parameters, often shortened to  $C_T$  and  $C_P$  respectively. Paterson gives  $C_T$  as  $\approx -1.0 \text{m } ^\circ\text{C}^{-1} \text{yr}^{-1}$  and  $C_P$  as  $\approx 1.0 \text{m m}^{-1} \text{yr}^{-1}$ .  $C_P$  increases above 1.0 when avalanching is a major mass input to the glacier, and below 1.0 when a significant portion of the precipitation flux is rain.

Under the assumption that contributions to the glacial **basin** balance from avalanching and melting from rain are negligible, equation 2.4 simplifies to.

$$\Delta M = c_P \cdot \Delta T + \Delta P \quad (2.5)$$

Because  $P$  is considered a flux in this paper, equations 2.5 and 2.2 can be combined to produce 2.6.

$$C_P \cdot \Delta T + P + \Delta G + \Delta B = Q + E \quad (2.6)$$

where the two  $P$ 's combine into an overall precipitation input.

The  $\Delta T$  remains problematic, as no reference steady-state mass balance data for these glaciers exist. 2.4 does assert that a linear relationship exists between glacial melt and mean melting season temperature. We can then assume:

$$C_P \cdot \Delta T = g \cdot T \quad (2.7)$$

Where  $g$  is now understood to be a melting constant, unique for each basin within our study area. We will assume further that  $g$  depends on the fraction of permanent-ice cover  $a_i$  within each basin, and define  $g_0$  to be the ice melting parameter (2.8).

$$g = a_i \cdot g_0 \quad (2.8)$$

This linear relation between mean summer temperature and melt is a first order approximation; nonlinear behavior may be observed if the average temperatures diverge wildly from 0°C at the glacier elevation. Changes in glacial ice albedo or % cloud cover may also affect the coupling of temperature to melt. To simplify our analysis, these complicating factors are neglected.

### 2.1.6 Precipitation

Precipitation in the region is dominated by winter snow coming from moisture derived from the Pacific Ocean. Most precipitation occurs between the months of November and May; the resultant snowpack largely melts between June and September.

Regional and local orographic lift combined with rainshadow effects control the amount of precipitation that falls on the drainage [Rice, 2011]. Thus a precipitation model dependent on elevation is needed to estimate the true precipitation that falls on each basin. To this end, data collected by Rice [2011] will be used to develop a linear precipitation model which obeys equation 2.9.

$$P(z) = m \cdot z + b \quad (2.9)$$

Only the slope value  $m$  will be examined from Rice [2011]. The offset term,  $b$  varies based on the precipitation year and will be calculated using snow pillow data available from the meteorologic stations near the study area.

Once a precipitation vs. elevation model is created, the true precipitation input to the basin can be found using equation 2.10.

$$P = b + \sum_{i=1}^n m \cdot z_i \cdot w_i \quad (2.10)$$

Where subscript  $i$  represents each elevation bin,  $z_i$  represents the midpoint elevation of each elevation bin,  $n$  is the number of elevation bins, and  $w_i$  is the fractional area each elevation bin represents within the basin. Note that offset  $b$  will vary each year depending on the amount of snowfall.

One complicating factor is the presence of monsoonal moisture during the summer months, which almost entirely falls as rain. Not only does rain not add to the glacial balance, it often facilitates the melt of glacial ice and snow. Although this moisture is not a significant fraction of yearly precipitation [Tangborn, 1977, Dean, 1974], it is a potential source of error.

### 2.1.7 Runoff

Runoff is the major outward flux of water from the basin system, removing all water that does not get transpired, stored in soil, or accumulated in the glaciers in the form of rivers and streams. To measure total runoff for the hydrologic year, discharge ( $\text{m}^3 \text{s}^{-1}$  of water) must first be measured at relevant field locations.

Discharge ( $q$ ) in a stream is equal to the average water velocity ( $u$ ) times the stream's cross section ( $a$ ).

$$q = u \times a \quad (2.11)$$

It is impractical to measure average water velocity continuously in a wilderness setting, but there exist many empirical equations which can approximate it based on river depth. One such equation is the **Manning Equation 2.12** which relates the average water velocity to local slope, bed roughness, and average stream depth:

$$u = \frac{Y^{\frac{2}{3}} \cdot S^{\frac{1}{2}}}{n} \quad (2.12)$$

where  $n$  is the channel conductance coefficient,  $Y$  is the average channel depth, and  $S$  is the local stream gradient ( $S = \frac{\Delta \text{Elevation}}{\Delta \text{Horizontal Distance}}$ ) [Dingman, 2002]. This can be further simplified by combining all non season-dependent variables into a channel coefficient,  $c$ :

$$u = c \cdot Y^{\frac{2}{3}} \quad (2.13)$$

Recognizing that  $Y$  is the vertical dimension of the stream, and that  $a = Y \times W$  ( $W =$  channel width), equation 2.11 becomes equation 2.14:

$$q = c \cdot Y^{\frac{5}{3}} \cdot W \quad (2.14)$$

Pressure sensitive instrumentation placed at the bottom of the river sites will not provide  $Y$  directly (due to pressure differences in elevation, pool depths, etc;) necessitating an offset to the measured stage/river depth data.

$$q = c \cdot (Y + \alpha)^{\frac{5}{3}} \cdot W \quad (2.15)$$

All stream sites where discharge data is to be calculated are then visited periodically and discharge is estimated empirically using hydrologic methods. A stage vs. discharge curve is then made by adjusting parameters  $\alpha$  and  $c$  in equation 2.15 to fit the empirically determined discharge data at instrument-recorded stage values. This curve is then used to transform the stage time series data  $Y(t)$  to a corresponding discharge series  $q(t)$ .

Since this study will only consider yearly hydrologic balances, it is necessary to integrate the discharge calculated by equation 2.15 over the hydrologic year. Dividing the resultant water volume by the area of the basin gives the total runoff in units of  $\text{m}^3/A$  :

$$Q = \frac{\int_{t_0}^{t_1} q(t) dt}{A} \quad (2.16)$$

Where  $t_0$  and  $t_1$  represent the beginning and end of the hydrologic year and  $A$  is the total basin area. The integral itself is numerically calculated by trapezoidal integration.

### 2.1.8 The Basin Water Balance Equation

With the prior justifications for zero groundwater input and ablation terms, evaporation dependence on evaporative area, and a linear relationship between glacial melt and mean summer temperatures, we now have equation 2.17, which will be used as an overall water balance equation for all basins in this study.

$$a_i \cdot g_0 \cdot T + P = Q + a_e \cdot e_0 \quad (2.17)$$

## 2.2 Available Instruments and Data

The following equipment and datasets are available to be used in this study:

- Three Meteorologic stations
- Several Solinst Barologger Golds
- Lyell, Maclure, and Tuolumne River Discharge Datasets
- Park Cover Map

### 2.2.1 Meteorologic stations

Three Meteorologic stations run by the [California Department of Water Resources/Snow Surveys](#) lie close to the study site:

- Tuolumne Meadows Meteorologic station
- Dana Meadows Meteorologic station
- Gem Pass Meteorologic station

The Tuolumne Meadows MET<sup>1</sup> station (station id:TUM) has been in place since 1930 and has been collecting hourly and event-based data on temperature, precipitation, wind-speed, and many other environmental variables. For the purposes of this study, only hourly adjusted snow water equivalent depth (sensor 82) and hourly temperature records (sensor 30) will be used. Only data from 08/01/2001 to 09/14/2014 will be included. Owing to several missing values and oscillations between negative and positive values during the summer, only the maximum value of snow water equivalent during the winter will be used during calculation of the  $b$  offset in equation 2.10. Hourly temperature data will be used in equation 2.17 to calculate glacial melt, as its temperature record is the most stable of all stations considered. This station is located 5km from the study site at 2600m above sea level.

The Dana Meadows MET station (station id:DAN) has been in place since 1926 and has been collecting hourly and event-based data on temperature, precipitation, wind-speed, and many other environmental variables since 1980. Of these, only daily adjusted snow water equivalent (sensor 82) will be used. Only the data between 08/01/2001 and 09/14/2014 will be used. The maximum value of sensor 82 will be used to calculate the  $b$  offset with equation 2.10. This station is located only 7km from the study site at 2980m above sea level.

The Gem Pass MET station (station id:GEM) has been in place since 1931 and has been collecting hourly and event-based data on temperature, precipitation, wind-speed,

---

<sup>1</sup>The word 'Meteorologic' in this study will be abbreviated as MET (example: Tuolumne Meadows MET station).

and many other environmental variables since 1985. Sensor 82, daily adjusted snow water equivalent will be used from this station to calculate  $b$  in equation 2.10. This record extends back to 11/09/1983, but only the period of time between 08/01/2001 and 09/14/2014 will be used. This station is located less than 10km from the study site at 3270m above sea level, and is the closest of the three stations to the glaciers. However it lies east of the Sierra Nevada crest and may exhibit rainshadow effects.

### 2.2.2 Solinst Levellogger Gold

The Solinst Levellogger Gold piezoelectric loggers are small cylindrical tubes 22mm x 154mm [Solinst Instrument Manuals]. They have the ability to record ambient pressure to within  $\pm 0.3$ cm water head equivalent and temperature once every minute for ten years without any maintenance or recharging. Since they are also watertight, they can be placed in stream beds where the pressure reading then corresponds to the water pressure head above the logger, known as stage.

Loggers were placed within low turbulence pools at locations shown on map 2.3. Each site's stage vs. discharge curve is produced by measuring discharge with the salt slug discharge method [Dingman, 2002], and by the transformations outlined in section 2.1.7.

Additionally a Solinst Barologger Edge was kept at a field station in Tuolumne Meadows to measure ambient barometric pressure. These data were directly subtracted from the logger data to correct for variations in atmospheric pressure.

### 2.2.3 Upper and Lower Twin Bridges Discharge Datasets

The hydrology team working for the Resource Management and Science Division of Yosemite National Park provided unpublished stage and discharge data for this study from three locations within the study area [National Park Service, Unpublished Hydrologic Data]. At Twin Bridges near Tuolumne Meadows, hourly discharge data is available from August 2001 through May 2014. Where the melt waters from Lyell and Maclure Glacier combine, two loggers have been recording discharge data since September 2012. One of these loggers is located just downstream from the Lyell-Maclure Creek confluence, and another has been placed approximately 400 meters upstream on Maclure Creek. Corresponding Lyell Creek flows above the confluence can be derived by subtracting the Maclure Creek dataset from the Lyell Creek data. These RMS logger locations are shown on figure 2.3.

The RMS data required the defining of the hydrologic year to extend from September 15th 1:00 to September 14th 24:00, with the ending date used as the year index. As a

---

consequence, no cumulative hydrologic data will be used from the Twin Bridges location for the 2014 hydrologic year.

## 2.2.4 Park Cover Map

A breakdown of the study basins by cover type is necessary to calculate contributions from glacial melt and evaporative losses. In 1997, YNP published a comprehensive vegetative cover map utilizing a mixture of areal surveys and field measurements [National Park Service]. This map contains data on surface cover, dominant species, and understory vegetative information. For each basin in the study area, surface cover was grouped into five categories. Each pixel on the map was placed under the major category according to the dominant cover present:

- **Forest**
  - Whitebark Pine
  - Sierra Lodgepole
  - Mountain Hemlock
- **Meadow**
  - Alpine Snowpatch Communities
  - Sierra Willow / Swamp Onion
  - Shorthair Sedge
  - Intermittent to Seasonally flooded meadow
  - Semi-permanently to Permanently flooded meadow
- **Water**
  - Water
- **Rock**
  - Alpine Talus
  - Alpine Scree
  - Mesic Rock Outcrop
  - Boulder Field
  - Sparsely to Non-vegetated Exposed Rock
- **Ice**

– Alpine Permanent Snowfield/Glacier

After placing each pixel into one of the above categories, percent cover of the basin was then derived by dividing each pixel count by total pixels contained in the basin. A summary of the cover types for each basin within the study area is presented in 2.2.

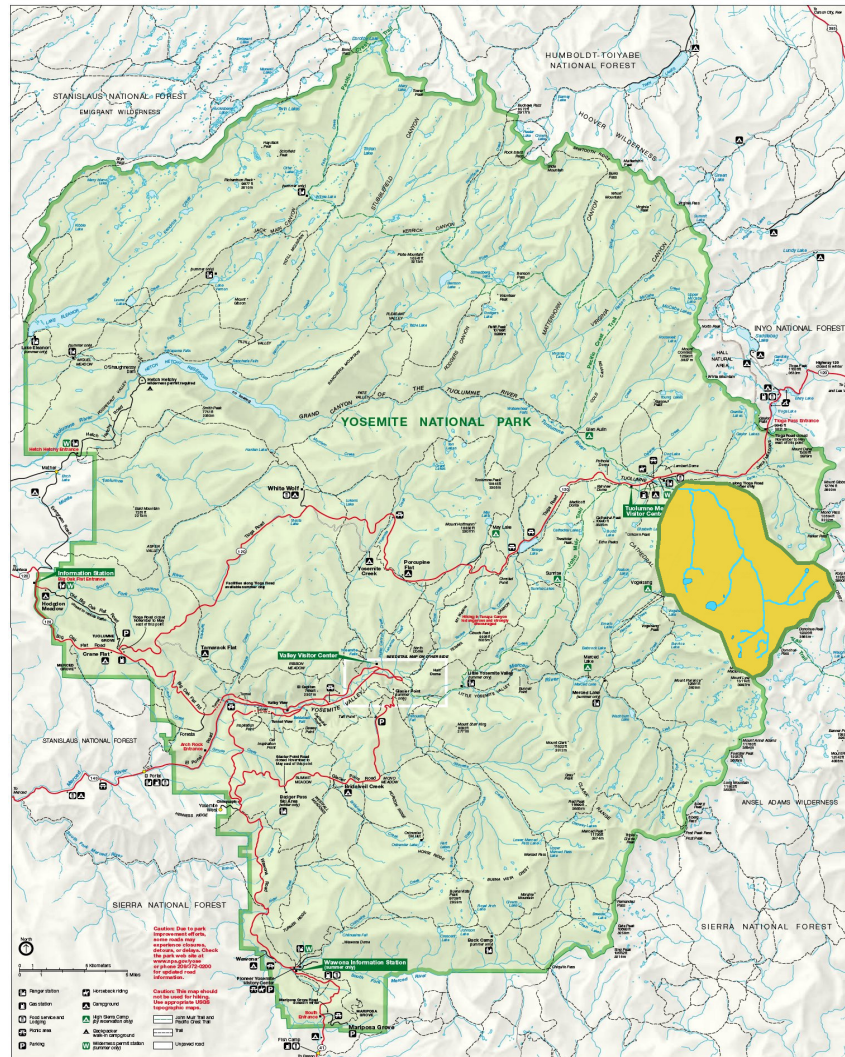


FIGURE 2.2: Study site within Yosemite National Park  
Highlighted region shows the study site in relation to Yosemite National Park.

## 2.3 Study Area Characterization

Refer to figures 2.2 and 2.3 for maps of the relevant study basins. Basin cover type and total area are summarized in tables 2.2 and 2.3.

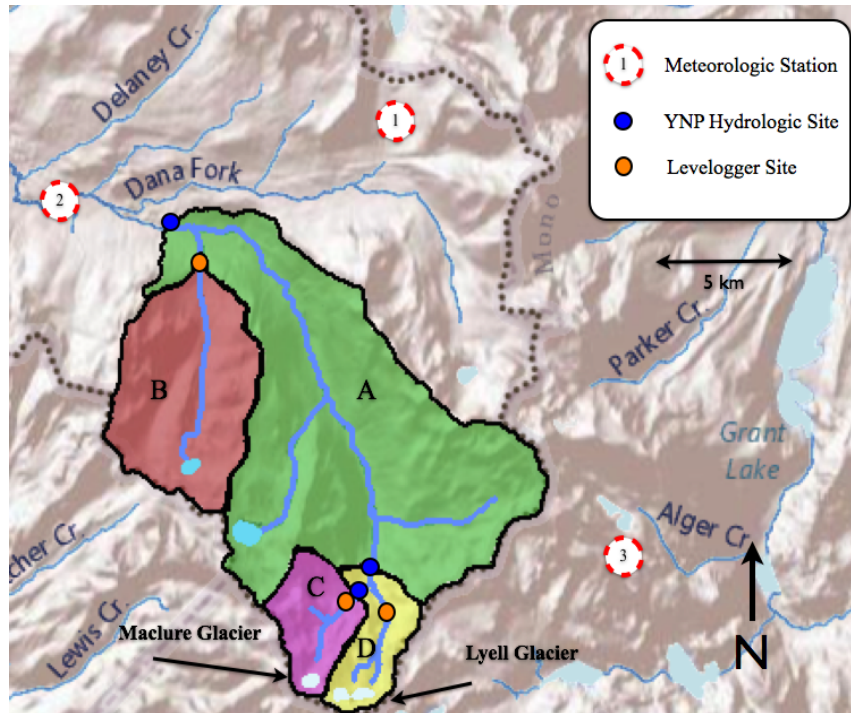


FIGURE 2.3: Study Basins and Important Locations

Shown are the four basins considered in the study. Area A is Tuolumne FATB Basin, area B is Rafferty Creek Basin, area C is Maclure Creek Basin, and area D is Lyell Creek ABVC Basin. Note that A also contains the areas of B, C, and D. Area D and C comprise Lyell Creek BLWC Basin. The three MET stations are also shown as white dots with broken red outlines. 1 corresponds to Dana Meadows MET station, 2 corresponds to Tuolumne Meadows Met station, 3 corresponds to Gem Pass Met station. Small blue circles are locations where hydrologic discharge data was gathered by the RMS division of YNP. Small orange circles are locations where the Solinst leveloggers were deployed.

### 2.3.1 The Lyell Fork of the Tuolumne River

The Lyell Fork of the Tuolumne River begins as snowmelt from the Lyell Glacier at 3600m. It then flows 13 km NE in a roughly straight line, making a sharp bend west at about 3 km from its confluence with the Dana Fork. Above its confluence with Dana Fork, the Lyell Fork is the second most heavily vegetated basin in the study area, with more than 70% of its area either Forest or Meadow. Upstream from the discharge loggers at twin bridges, the Lyell Fork drains 109km<sup>2</sup>. This area will be referred to in this study as the Tuolumne Fork above Twin Bridges (Abbreviation Tuolumne FATB).

<b>Basin</b>	<b>Forest (%)</b>	<b>Meadow (%)</b>	<b>Water (%)</b>	<b>Rock (%)</b>	<b>Ice (%)</b>
Tuolumne FATB	57.01	14.59	1.09	26.03	1.28
Rafferty Creek	75.56	9.40	0.83	14.17	0.04
Lyell Creek BLWC	14.54	14.46	1.57	60.79	8.63
Maclure Creek	9.75	15.46	2.18	65.03	7.57
Lyell Creek ABVC	19.37	13.46	0.96	56.51	9.71

TABLE 2.2: Basin Percent Cover Type  
Comparison of basin cover types according to definitions given in section 2.2.4.

<b>Basin</b>	<b>Total Area (km<sup>2</sup>)</b>	<b>E Area (km<sup>2</sup>)</b>	<b>Ice Area (km<sup>2</sup>)</b>
Tuolumne FATB	109.2	79.4	1.397
Rafferty Creek	24.55	21.06	0.009
Lyell Creek BLWC	15.29	4.67	1.319
Maclure Creek	7.68	2.1	0.581
Lyell Creek ABVC	7.61	2.57	0.739

TABLE 2.3: Basin Area by Percent Cover Type  
ARCGIS along with the [National Park Service](#) was used to break down each of the basins used in the study by cover type. Cover types were then used to estimate external water fluxes to the atmosphere and glacial melt constants. Column *E Area* denotes assumed area available for all major evaporative fluxes to occur as outlined in section 2.1.2.

### 2.3.2 Maclure Creek

Maclure Creek originates on the Maclure Glacier, nestled between Mt. Florence and Mt. Maclure at an elevation of 3600 m. it flows through a series of flat meadows and cascades till it joins up with Lyell Creek at BLANK meters of elevation. Above its confluence, Maclure Creek drains 7.7km<sup>2</sup>. This area will be referred to in this study as Maclure Creek.

Most of the Maclure Creek drainage surface cover (65.0%) is classified as rock, therefore this basin is expected to exhibit the least amount of evaporative losses of all basins considered.

### 2.3.3 Lyell Creek Below Confluence

Lyell Creek originates on the Lyell Glacier, shaded by Mt. Lyell and Mt. Maclure. from below its confluence with Maclure Creek, Lyell Creek drains 15.3km<sup>2</sup>. The majority (60.8%) of the drainage cover is classified as rock, thus this basin is expected have low rates of evapotranspirative losses. This area will be referred to in this study as Lyell Creek below confluence (Abbreviated as Lyell Creek BLWC).

### 2.3.4 Lyell Creek Above Confluence

Lyell Creek above its confluence with Maclure Creek does not have any stable loggers to directly record the discharge contribution from the Lyell Creek Basin, but a discharge record can be inferred by subtracting Maclure Creek's discharge record from the Lyell Creek Record. This inferred basin has an area approximately the same size as Maclure Creek of  $7.61\text{km}^2$ , with similar surface cover statistics. This area will be referred to in this study as Lyell Creek above confluence (Abbreviated as Lyell Creek ABVC).

### 2.3.5 Rafferty Creek

Rafferty Creek is unique from the upper Lyell Creek and Maclure Creek Basins in that it very little perennial ice cover, as well as having the highest percent potential evaporative area of the basins  $> 85\%$ . It meets the Lyell Fork of the Tuolumne River within a few hundred meters of the RMS Twin Bridges logger site, and encompasses  $24.6\text{km}^2$ . This area will be referred to in this study as Rafferty Creek.

Because of its proximity to both Maclure and Lyell Creek ABVC and its lack of perennial ice cover, Rafferty Creek presents itself as an ideal control basin.

## 2.4 Possible Complications

Because of the high elevation, climate, and management concerns relevant to the study area, several potential challenges exist with obtaining and interpreting the data.

### 2.4.1 Cold Temperatures

During the winter months, temperatures at some of the logger sites may drop to  $-30^\circ\text{C}$ . Freezing water on the surface of small streams can lead to inconsistencies in the relation between observed pressure and weight of the water column directly above the logger. It is hoped that the largely corrected discharge data from YNP's RMS division can assist in the identification and correction of freezing related data anomalies.

Cold temperatures may also affect the electronics in the logger. It was unknown prior to the survey if cold temperatures would be experienced by the loggers during the study duration.

### 2.4.2 Timing of Spring Pulse

Ideally stage vs. discharge curve data would be collected at all levels of a river's flow, especially during the high spring pulse and late season low flows. Environmental conditions during the expected spring pulse are often hazardous to researchers, limiting the extend of empirical stage vs. discharge data. If large events are observed that exceed the range of empirical data, equation [2.15](#) must be extrapolated beyond the empirically observed discharge bounds.

## Chapter 3

# Data Analysis

### 3.1 Logger Complications

During the course of data analysis, the deployed loggers produced unexpected pressure spikes, changes in logger baselines, and high frequency-high amplitude behavior that could not be easily explained through hydrologic processes typical of the study site. This was troubling because these leveloggers contain the only data from Lyell and Maclure creeks prior to 2012. Ultimately it was determined that the data from the leveloggers was not reliable enough to be considered for analysis. Section 3.1.1 is therefore devoted to analyzing why the data was errant as well as suggestions for future studies utilizing Solinst Leveloggers.

#### 3.1.1 Suspicious Data

##### 3.1.1.1 Expected Data Trends

If it is assumed that the deployed leveloggers correctly record river stage, three key signals should be present:

- A diurnal cycle
- A large spring pulse
- Minimal flows during late summer, fall, and early winter.

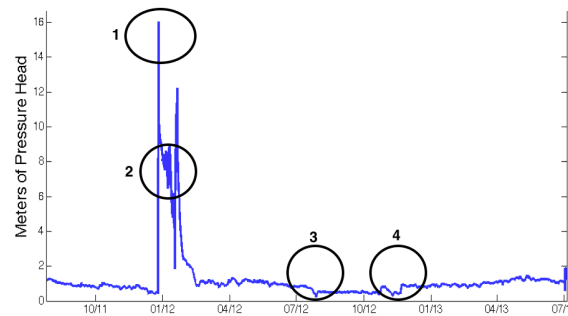
Diurnal cycles are caused by variations in solar radiation input on snowpack as the sun progresses across the sky. They should be visible as cycles with a 24 hour period.

Spring pulses arise from increased seasonal temperatures melting the accumulated winter snowpack. The majority of river discharge should occur sometime between April and June, manifesting itself in this large spring pulse.

Of great importance to this study are the low flows observed after the majority of snowpack has been melted. These flows may contain the majority of permanent ice loss discharges and as such are crucial to accurately measure.

Three representative logger timeseries have been picked to illustrate the levellogger's deviation from these expected signals; Rafferty Creek, Maclure Creek, and Lyell Creek ABVC. All three of these loggers exhibit anomalous flow signals.

### 3.1.1.2 Rafferty Creek Logger



(A) Rafferty Creek Timeseries



(B) Rafferty Creek Logger Site

FIGURE 3.1: Rafferty Creek Logger Data

(A) Rafferty creek levellogger time series. Each circle and number highlights suspicious data. (B) The Rafferty Creek levellogger location. Stream is approximately 6m wide. YNP geologist Dr. Greg Stock stands at  $\approx 2$ m.

The Rafferty Creek Logger, plotted in figure 3.1a, exhibits four anomalous data trends which bring into question the ability of this logger to reliably record river stage.

The first anomaly is an extremely large pressure head, equivalent to 16 meter of water column above the logger (labeled 1 in figure 3.1a). Prior to this, the logger reads a water column height of  $\approx 0.3\text{m}$ , with the logger reaching maximum pressure one hour later. Aside from a truly extreme precipitation event (which is not evident in any of the meteorologic station records), both the pressure change rate and the absolute pressure spike are likely impossible for the logger site to experience. A photo of the logger site 3.1b reveals that the creek can support about  $\approx 3\text{m}$  of vertical water column before spilling over its levees.

The second anomaly consists of a series of high-frequency oscillations between 12m and 2m of vertical water pressure equivalent (labeled 2 in figure 3.1a). Diurnal cycles are to be expected in water runoff time series, but the magnitude of fluctuations much larger than would be expected from changes in average temperature and radiation flux between night and day.

From early August 2012 through mid October 2012, Rafferty Creek was reported as completely dry by YNP staff. If the logger was functioning correctly it should have recorded a flat, static record for the period. Yet the logger clearly exhibits a gradual slump into a near-zero value, followed by an increase up to a static value that is maintained till mid-winter (labeled 3 in figure 3.1a).

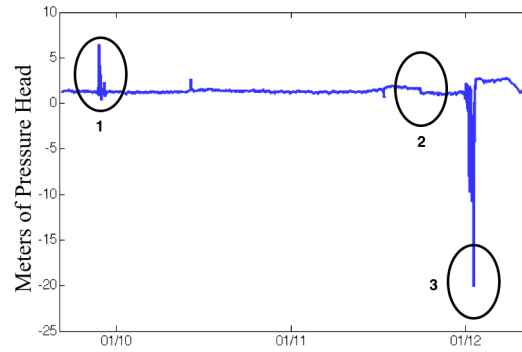
Finally, this logger records a step change which takes place over the course of a week in January (labeled 4 in 3.1a). While the magnitude of the anomaly falls within the natural variation of the expected stage, it is difficult to account for any physical process which may be responsible for the step change.

Aside from these anomalies, the Rafferty Creek Logger does exhibit small spring pulse events, decreased stream heights during times when the snowpack is known to be depleted, and diurnal cycles during snowpack melt, which are consistent with expected logger behavior.

### 3.1.1.3 Maclure Creek Logger

The Maclure Creek Logger, plotted in figure 3.2a, exhibits three anomalous data trends which bring into question the ability of this logger to reliably record river stage.

Similar to the #1 anomaly in 3.1a, a much larger-than expected pressure magnitude and gradient was seen during early winter 2010 in the Maclure Creek Logger. Labeled 1 in 3.2a, it has a maximum amplitude equivalent to 5m of vertical water column, something completely impossible given the creek cross section in 3.2b. During an expedition to the logger site in September 2014, debris deposited from a flood the month before was found



(A) Maclure Creek Time Series



(B) Maclure Creek Logger Site

FIGURE 3.2: Maclure Creek Logger Data

(A) Maclure Creek Logger data. Each circle and number highlights suspicious data.

(B) The Maclure Creek Logger was placed in a meandering meadow stream with stream banks  $< 1\text{m}$  high. Tree visible on the left in the background is  $\approx 2\text{m}$  high.

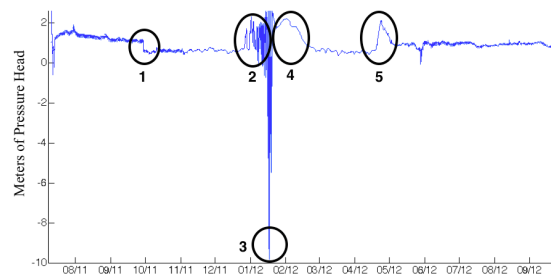
resting approximately 2 vertical meter above the bottom of Maclure Creek, but this was attributed to a unusually intense rainfall event occurring due to monsoonal moisture. Because anomaly 1 occurred during the winter of '09-'10, no known precipitation event could be responsible for this particular spike.

Also similar to the #4 anomaly in 3.1a, the Maclure Creek Logger exhibits a downward step change in the data just prior to December 2011 (labeled 2 in figure 3.2a). The cause of this step change is unknown.

Curiously, the Maclure Creek Logger also exhibits an unusual negative pressure spike of  $-20\text{m}$  (labeled 3 in figure 3.2a). Such negative pressure spikes are nonphysical if the logger is assumed to record absolute pressure.

Quickly after this negative pressure event, a small bump of  $\approx 1\text{m}$  is observed that corresponds to the spring pulse. Diurnal cycles are also observed in between these anomalous data.

### 3.1.1.4 Lyell Creek



(A) Lyell Creek Above Confluence Logger Time Series



(B) Lyell Creek Above Confluence Logger Site

FIGURE 3.3: Lyell Creek Above Confluence Logger Data

- (a) Lyell Creek ABVC time series. Each circle and number highlights suspicious data.  
 (b) The Lyell Creek Logger was placed in a sparsely forested area downstream of Lyell Glacier. Glaciologist Dr. Robert Anderson is visible gauging stream height and stands at just below 2m of height.

The Lyell Creek Logger exhibited the most unexpected phenomena of any of the loggers employed. Step changes, high frequency-high amplitude changes, extreme negative spikes, and anomalous high bumps were observed in the data [3.3a](#).

The first anomaly consists of a step change of approximately 0.5m of pressure change, which occurred mid-October 2011. This change occurs over a single hour and is the only step change present in the time series.

The second anomaly consists of high frequency-high amplitude pressure variations which range from nearly 2m ending with the third anomaly's  $-10\text{m}$  pressure spike. This again occurs in the middle of winter. Neither the pressure high of 2m can possibly be explained by 2m of water column as evidenced by the lack of debris around the trees at this height, and the presence of many small saplings which would be damaged by such flows [3.3b](#).

A negative pressure spike similar to figure 3.3a's negative pressure spike is also visible, but with a lower amplitude of around  $-10\text{m}$ .

Immediately after the large negative spike, a large bump with a maximum value of  $2\text{m}$  is observed (labeled 4 in figure 3.3a). This bump exhibits no diurnal cycle and is of an unusually long wavelength compared to the rest of the data. A similar feature, labeled 5, is also visible with similarities to anomaly #4 and occurs approximately when the spring pulse would be expected. While  $2\text{m}$  of vertical water may seem more realistic for this location, the lack of debris around the logger site at the  $2\text{m}$  flow level does not substantiate anomalies 4 and 5 as representative of true flows.

### 3.1.2 Potential Physical Explanations

If the observed anomalies were due to purely physical processes, then there is hope that portions of the record could be corrected to better reflect the true stage. Three possible hydrologic processes were considered, and while some of the processes could mimic some of the observed data, they ultimately failed to account for all of the anomalies.

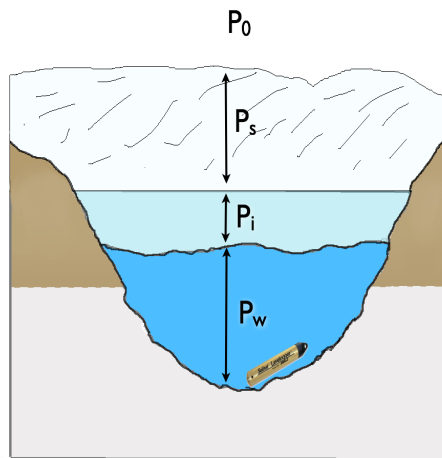


FIGURE 3.4: The Expanding Ice Hypothesis

Illustrated above is the expanding ice hypothesis. The Logger records a combination of expanding ice  $P_i$ , water column  $P_w$ , piled snow  $P_s$ , and ambient pressure  $P_0$ .

One of the hypothesis for greater than expected flow heights is the formation and expansion of ice at the logger location. In this scenario, extreme cold temperatures cause the logger to be isolated from the rest of the stream via ice expansion. As the ice continues to expand into the liquid water pocket, it places pressure on the underlying liquid, causing the logger to read a higher pressure than would be caused by the equivalent height

of liquid water. Additional pressure could be created from thick snow drifts amassing on top of the frozen stream. See figure 3.4 for an illustration.

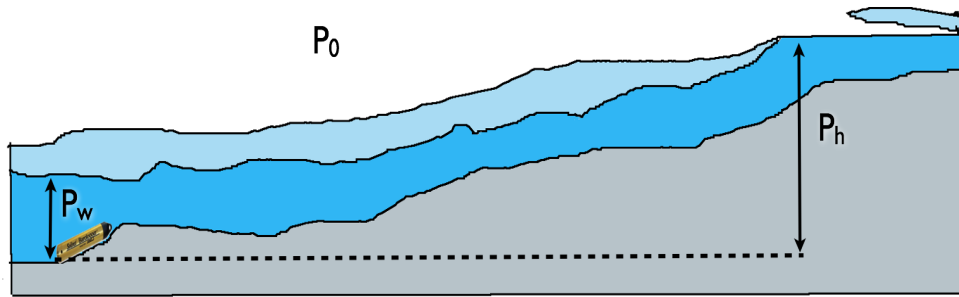


FIGURE 3.5: The Ice Pipe Hypothesis

A hard rind of ice on the surface of a stream can cause the installed logger to record the pressure head of  $P_h + P_0$  rather than  $P_w + P_0$ . Note that  $P_h$  depends only on elevation to nearest unfrozen upstream location.

Another hypothesis explains the anomalously high flow records by assuming a winter stream's surface is covered by a stable layer of ice. This ice covering can transfer the pressure head of an uncovered portion of water upstream of the logger to the logger site, similar to how gravity-fed water towers work in towns. This is known as the 'Ice Pipe' hypothesis and is illustrated in figure 3.5.

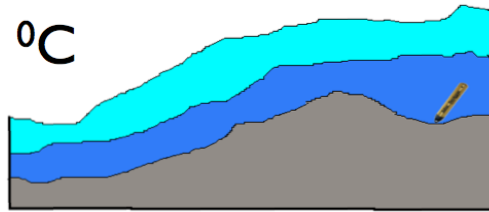
Negative pressure spikes are far harder to explain with simple ice expansion, but one hypothesis for these extreme negative spikes is based on pressure dependence on temperature. Initially the logger is assumed to occupy a small pool of water which is isolated from the environment by a hard ice shell. Some disturbance (example: a falling branch) causes the lower end of the ice shell to breach and allows the water within the pocket to drain. The breach then refreezes, trapping the logger in a pocket of air. This process is illustrated in figure 3.6.

Assuming an adiabatic lapse rate of  $5^\circ\text{C}/\text{km}$  and using minimum temperatures in records from nearby Yosemite Valley, the loggers have the potential to experience temperatures of  $-32^\circ\text{C}$  during the winter. By the  $P \cdot V = n \cdot r \cdot T$  ideal gas law, a drop in temperature within a finite volume leads to a drop in pressure.

A MATLAB script was written to examine the pressure drop within a volume of 1 liter assuming initial and final temperatures of  $0^\circ\text{C}$  and  $-32^\circ\text{C}$ . As illustrated in figure 3.7 negative pressures were produced, but they were of a much smaller magnitude than what the loggers recorded in figure 3.2a and figure 3.3a.

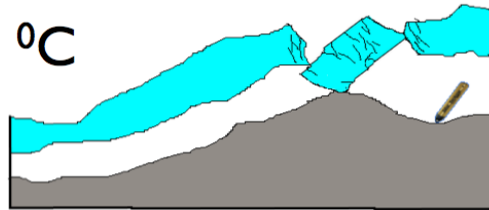
$$P = P_w + P_i + P_0$$

$$T = 0 \text{ } ^\circ\text{C}$$



$$P = P_0$$

$$T = 0 \text{ } ^\circ\text{C}$$



$$P < P_0$$

$$T < 0 \text{ } ^\circ\text{C}$$

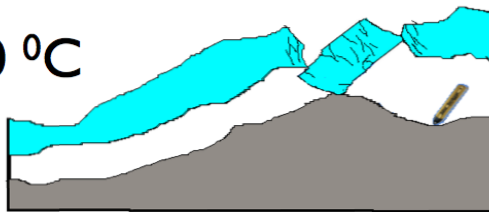


FIGURE 3.6: The Negative Pressure Hypothesis

First, a hard rind of ice forms on the surface of the stream. Next, a disturbance causes the rind to break and refreeze, trapping the logger inside a pocket of air. Water exits the logger location either through draining or by flowing out through underlying alluvium. As the temperature continues to fall, the logger records a negative pressure via  $PV = nrT$ .

### 3.1.2.1 Freezing Experiment

While the Ice Pipe hypothesis was not testable in the field due to the hazards of winter fieldwork, nor in the lab due to lack of equipment, an experiment was conducted with a logger placed in a freezer to mimic the extreme winter conditions at the logger site.

The logger was first submerged in 30cm of water contained within a beaker, then placed inside a freezer capable of reaching  $-30^\circ\text{C}$ . Simultaneously, a barometric logger was placed alongside the submerged logger to record changes in ambient pressure. Both the

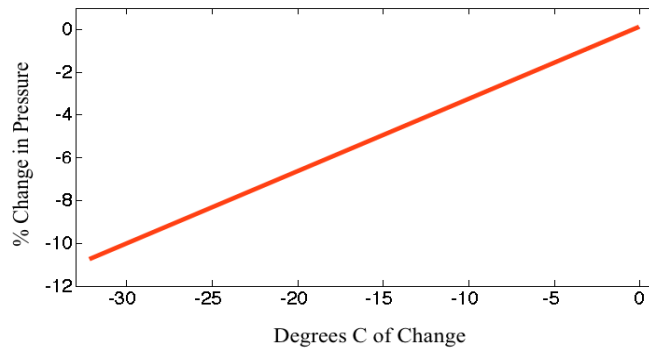


FIGURE 3.7: Matlab Negative Pressure Simulation

Using a 1 liter volume beginning at ambient barometric pressures experienced at 3km of altitude, changes in pressure were calculated by gradually reducing temperature down to  $-32^{\circ}\text{C}$ . Y axis is calculated as  $1 - P_{final}/P_{initial}$ .

barometric logger and the submerged levellogger were kept in the freezer overnight, then removed and left to thaw for a day. Figure 3.8 displays the results.

The barometric logger record 3.8a notably exhibited extreme negative pressure dips impossible for the freezer to contain. Even after the logger had equilibrated temperature-wise with the atmosphere after it was removed from cold temperatures, the pressure anomaly never fully returned to ambient pressures.

The uncompensated record 3.8b exhibited a 50cm spike in recorded pressure, followed by a sharp, deep  $-2.5\text{cm}$  dip vs. initial pressure level. After its removal from the freezer, it rapidly returned to near-previous recorded pressure levels.

By subtracting the barometric logger's values from the levellogger's, the true pressure head above the levellogger should be obtained 3.8c. The corrected record exhibits elements of both the barometric logger's extreme negative spikes and the large positive spikes recorded from the uncompensated levellogger record.

By subjecting both the levellogger and barometric logger to freezing conditions representative of temperatures in the field, rapid negative spikes, positive spikes, and gradual step-like changes were produced. In this experiment it was shown that cold temperatures affect both the barometric logger, and the effective water column height recorded by the levellogger.

### 3.1.3 Logger Methodology Conclusions

The data recorded by the deployed levelloggers may still be valuable, but in light of the results obtained from the freezing experiment there seems to be no simple way of

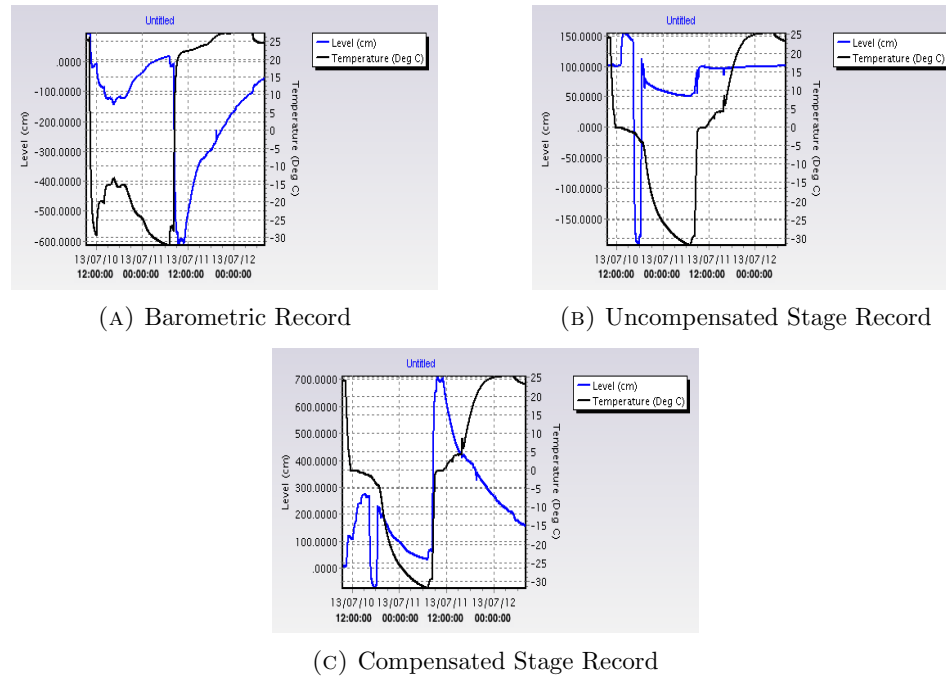


FIGURE 3.8: The Freezing Experiment

Record 3.8a shows temperature and pressure readings taken from the barometric logger as it was frozen and thawed alongside its submerged counterpart. Record 3.8b shows the uncompensated levellogger data as it was frozen and thawed under 30cm of water. Record 3.8c shows the Logger data subtracted by the ambient pressure recordings of 3.8a.

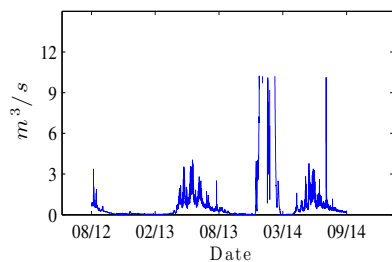
correcting these data. Anomalously high and low values can be produced by a combination of cold temperatures affecting the reliability of the loggers and the conditions they experience while in freezing water. This finding was further corroborated by the [Solinst Instrument Manuals](#), which explain that the sensor that records pressure consists of a capacitive diaphragm which could be damaged by expanding ice.

Any future studies attempting to gauge stream stage or discharge must be aware of potential winter conditions. Instrumentation which relies on pressure or direct contact with the water must be able to operate in ice choked streams and extreme cold temperatures. Although these data cannot be used for this study, they do highlight the need for improved field methods when gathering stream discharge data.

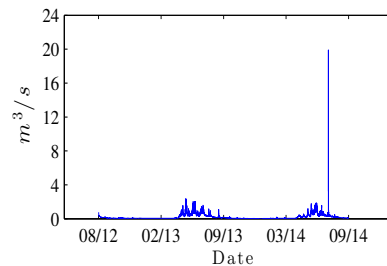
## 3.2 Discharge Dataset

Unlike the barometric and levelloggers placed specifically for this study, the Lyell Fork discharge data provided by the RMS division of YNP is extremely stable. Spring pulses,

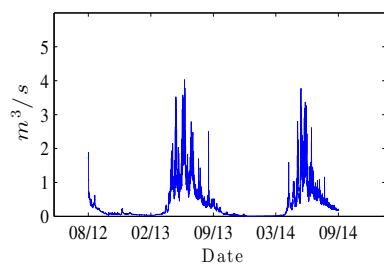
diurnal cycles, and minimal flows late season are evident from this data. Only two locations, Lyell Creek BLWC, and Maclure Creek exhibit anomalies that must be corrected before being used in the basin balance models.



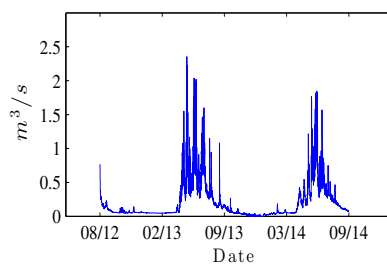
(A) Lyell Creek BLWC Raw Discharge Data



(B) Maclure Creek Raw Discharge Data



(c) Lyell Creek BLWC Data After Corrections



(D) Maclure Creek Data After Corrections

FIGURE 3.9: Lyell Creek BLWC and Maclure Creek Discharge Data

Subfigures 3.9a and 3.9b show the discharge dataset before corrections were applied. Immediately visible are the anomalously high flows around 7/16/2014 and inconsistent winter data for the 2014 hydrologic year. Subfigures 3.9c and 3.9d show the discharge data post correction; the anomalous monsoonal event is removed and the winter discharges are smoothed to near zero.

### 3.2.1 Monsoonal Event Correction

On July 16, 2014 starting at 3:30 pm, both the Lyell Creek BLWC and Maclure Creek data show a phenomenal jump in discharge. Within the course of an hour the Lyell discharge record increases from  $0.5\text{m}^3\text{s}^{-1}$  to  $10\text{m}^3\text{s}^{-1}$ . On the same day from 2:00 pm to 4:00 pm, the Maclure dataset shows an increase from  $0.25\text{m}^3\text{s}^{-1}$  to  $20\text{m}^3\text{s}^{-1}$ . Both flows return to pre July 16th 3:00pm flows exactly five days later.

Obviously a higher recorded discharge on Maclure creek than at Lyell Below confluence is not possible; discussions with the RMS department of YNP confirmed that a torrential rain occurred during this period which raised the stage of the river beyond the stage vs. discharge curve bounds used to calculate discharge.

Additionally since the basin model only deals with winter SWE precipitation input, both the Maclure and Lyell records from 3:00 pm July 16th, 2014 to 3:00 pm July 21, 2014

were deleted. Linear interpolation between these two times was used to fill in the gap of data.

During this monsoonal event, the minimal temperature recorded at Tuolumne Meadows MET Station (Elevation 2600m) by the [California Department of Water Resources/Snow Surveys](#) was 8.9°C. If we assume a lapse rate of 5.0°C/km, and consider that the glaciers are at 3660m, the temperature at the glaciers would be 3.6°C. This implies that there was likely rain falling directly on the glacial ice, potentially transferring a large amount of heat into the glaciers. By excluding this monsoonal event from the record, we unfortunately exclude the melt created from this event in our analysis.

### 3.2.2 Maclure and Lyell Discrepancies

During the winter months, the Lyell and Maclure discharge data show a dramatic decrease in flow. However there are times in the record where the Lyell Creek BWLC flow oscillates under  $< 0.1\text{m}^3\text{s}^{-1}$ , and the Maclure Creek discharge data records flows higher than the Lyell data.

Deriving the Lyell Creek ABVC from subtracting the Maclure Creek data from the Lyell Creek BLWC at this point will lead to areas in the record where the Lyell Creek ABVC data are negative. Therefore the records must be adjusted to reflect likely discharges. The following rules will be applied to adjust the Lyell Creek BLWC and Maclure Creek data for each time  $t_i$ :

- If the Maclure Creek Flow  $Q_m > \text{Lyell Creek BLWC } Q_l$ , Maclure Creek flow  $Q_m(t_i) = Q_l(t_i) \cdot 0.5$ . Lyell Creek BLWC drains approximately twice the area above the Maclure Creek Logger, so the 0.5 multiplicative term is reasonable during low flows.
- If the Maclure Creek Flow is non-zero when the Lyell Creek flow is zero, set the Maclure Creek flow to  $Q_m(t_i) = 0$ .

Any errors introduced by these rules should be made inconsequential by the small contribution winter discharge makes to the cumulative hydrologic year runoff. Figure 3.9 illustrates the Lyell BLWC and Maclure Creek discharge series pre and post corrections.

### 3.2.3 Twin Bridges Discharge Dataset

The Tuolumne FATB discharge data (figure 3.10) collected from the twin bridges station, in contrast to the Lyell Creek BLWC and Maclure Creek data, show no troubling

features. Regular spring pulses, diurnal cycles, and low winter flows are visible for the entire record. No monsoonal even correction is needed as the data is only available up to 6/10/2014.

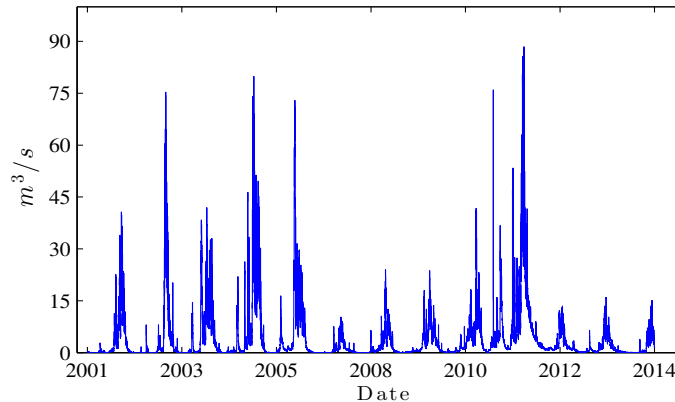


FIGURE 3.10: Discharge Series for Tuolumne Fork Above Twin Bridges  
The discharge time series for Tuolumne FATB required no correction for extreme monsoonal events or freezing conditions.

### 3.3 Precipitation Data

Rice [2011] utilized remote sensing to examine differences in snow melt timing between elevations within the Tuolumne River and Merced River basins. For the 2004-2005 hydrologic years, the data they examined showed distinct linear trends with a high degree ( $r^2 > .98$ ) of correlation. Two slope values were found after a linear regression; the 2004 linear fit had a slope of 1.99mSWE/kmEl with  $\sigma = 0.15\text{mSWE/kmEl}$  and the 2005 linear fit had a slope of 3.01mSWE/kmEl with  $\sigma = 0.21\text{mSWE/kmEl}$ . Rather than average out the mSWE/kmEl values, each slope value will be used to create a spread of possible precipitation input models.

#### 3.3.1 Precipitation Models

Initially, 18 precipitation models (3 basins x 3 meteorologic snow pillows x 2 slopes) were prepared according to equation 2.10. Figure 3.12 and 3.13 show the basin-averaged snow water equivalent precipitation inputs calculated for these models.

On all basins modeled, the Tuolumne Meadows MET Station-based models had a much larger variation in SWE, with different slope parameter resulting in almost a meter of SWE difference. Additionally the Tuolumne MET Station-based models show the

Hydrologic Year	2400-2700m	2700-3000m	3000-3300m	3300-3600m	3600m+
2004	0.31	1.01	1.68	2.88	3.86
2005	0.58	1.39	2.08	2.44	3.02

TABLE 3.1: Average Snow Water Equivalent depth Estimates by Elevation for the Tuolumne River

For each elevation bin, Rice [2011] averaged the accumulation within the bin to produce the snow water equivalent data seen in this table. All values are in vertical meters of water equivalent.

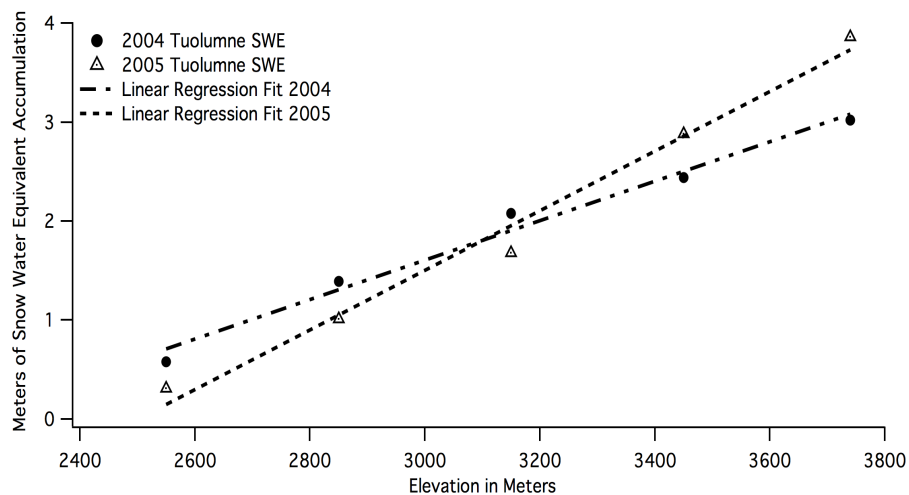


FIGURE 3.11: Snow Water Equivalent Elevation Trends

Data from table 1 of Rice [2011] plotted vs. elevation bin midpoint. 2004 linear regression fit has an  $r^2 = 0.983$ ; 2005 linear regression fit has an  $r^2 = 0.985$ .

highest average SWE. Variations between 'wet' years (2006, 2011) vs. 'dry' years (2007, 2014) are qualitatively less than the variation seen in Gem Pass MET Station models. This may be due to local orographic effects; the Tuolumne Meadows MET Station snow pillow does not have any large peaks to the west, the greater Tuolumne River basin outside the study area may tend to funnel storms towards the pillow, and the pillow itself is located in a topographical storm cloud "funnel" [Stock, 2015]. The exact magnitude and prevalence of local orographic effects in these data is beyond the scope of this study.

The Dana Meadows MET Station models exhibit qualitatively more variation in SWE per year than the Tuolumne Meadows MET Station models. Curiously, the large snow-pack year of 2011 [Western Regional Climate Center] evident in both the Gem Pass and Tuolumne Meadows-based models is not seen in the Dana-based models. For Tuolumne

FATB Basin, Lyell Creek BLWC Basin, and Maclure Creek Basins, the Dana-based models do not vary as much between slope parameter as do the Tuolumne MET Station-based models.

The Gem Pass MET Station models are spaced tighter than either of the two previous models. Both the wet years of 2011 and 2006 are evident in the Gem Pass models. It is notable that this model more often than not predicts the lowest precipitation values throughout all three basins. The Gem Pass station is located east of the Sierra Nevada crest, thus this low prediction may be the result of a rainshadow effect. Additionally while slope  $s_1$  tends to produce a higher precipitation average throughout all models considered, for the Tuolumne FATB Basin the Gem Pass MET Station model shows that a higher slope of  $s_2$  results in a lower average precipitation. This may be the result of GEM pass being located at a higher elevation than most of Tuolumne FATB Basin. Somewhat troubling, the GEM Pass models predict a negative snowpack in 2014 for the Tuolumne FATB Basin, a physical impossibility.

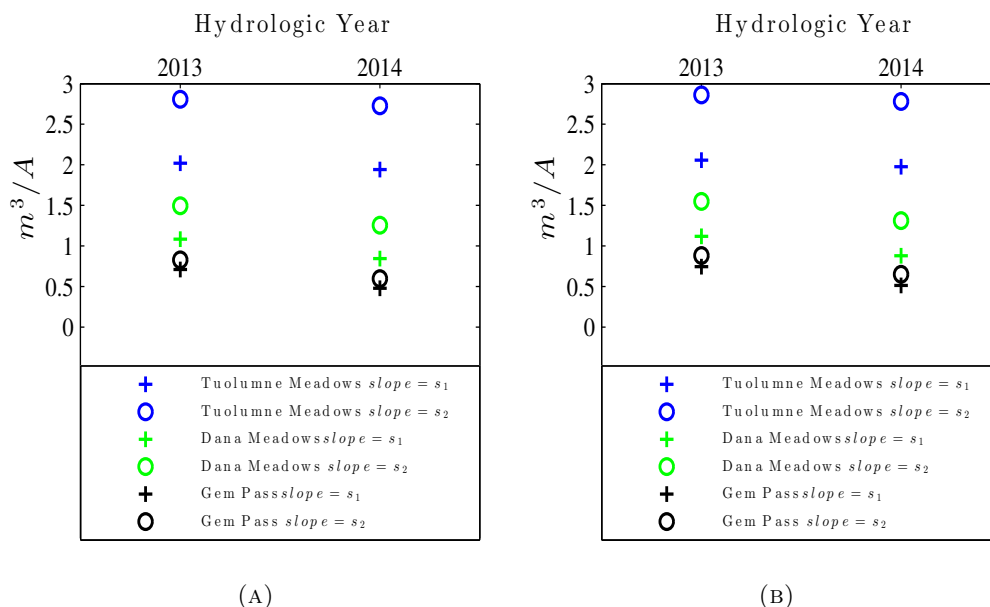


FIGURE 3.12: Lyell BLWC and Maclure Basin Precipitation Models. (A) shows the spread of precipitation models for Lyell Creek BLWC Basin. (B) shows the spread of precipitation models for Maclure Creek Basin. Y axis is in basin-averaged water depth (total water volume / basin area =  $m^3/A$ ). Two slopes were used in these models: slope  $s_1 = 1.99\text{mSWE/kmEl.}$  and slope  $s_2 = 3.01\text{mSWE/kmEl.}$  Precipitation models could have been calculated for years before 2013, but there is no corresponding discharge data from that time (see figure 3.9).

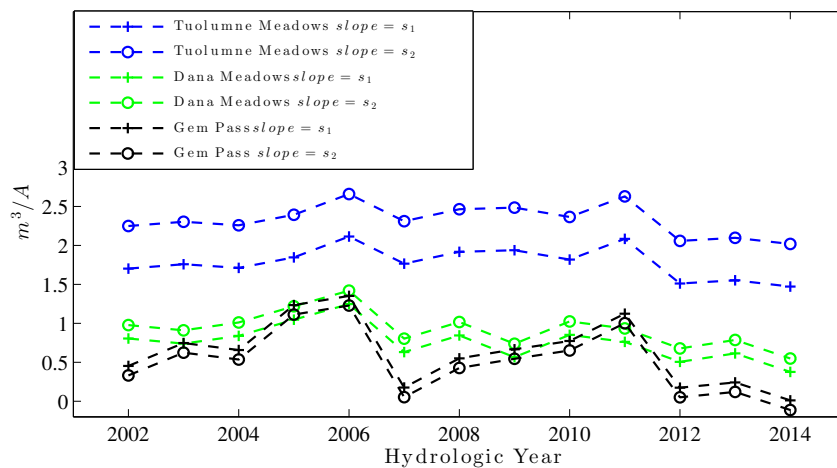


FIGURE 3.13: Precipitation Models for the Lyell Fork of the Tuolumne at Twin Bridges Site

Two slopes were used in the Tuolumne FATB Basin model: slope  $s_1 = 1.99\text{mSWE/kmEl.}$  slope  $s_2 = 3.01\text{mSWE/kmEl.}$  X axis is hydrologic year. Note that precipitation model extends to the 2014 hydrologic year, although no corresponding discharge data exists for that year (see figure 3.10).

### 3.3.2 Comparison With Discharge Data and Evapotranspiration

It is tempting to throw out the Tuolumne MET Station and Gem Pass MET Station models due to Tuolumne's large spread and Gem Pass's negative value during 2014. However these models should be judged on how well they conform to the discharge data discussed in earlier sections, as well as the plausibility of the resulting basin balance, ignoring contributions from groundwater.

For Tuolumne FATB Basin utilizing the Twin Bridges discharge dataset,  $E_{min} = 0.3m$  and  $E_{max} = 0.5m$ . Figure 3.14 compares the various precipitation models with cumulative discharge data.

For both the Lyell Creek BLWC and Maclure Creek Basins,  $E_{min}$  and  $E_{max}$  will be calculated based on evaporative area and the evaporation constants outlined in section 2.1.2. Figure 3.15 illustrates the precipitation-discharge comparison.

If any of the precipitation models for the Tuolumne FATB Basin reflected the true basin-averaged snow water equivalent input, at least one of the models should be seen to fall near or within the 0.3m to 0.5m discharge offset series. Instead, models seem to be a better fit for the Tuolumne FATB discharge data during different years:

- From 2003 to 2004 the Tuolumne MET Station-based model with slope =  $s_2$  seems to be an appropriate precipitation model.

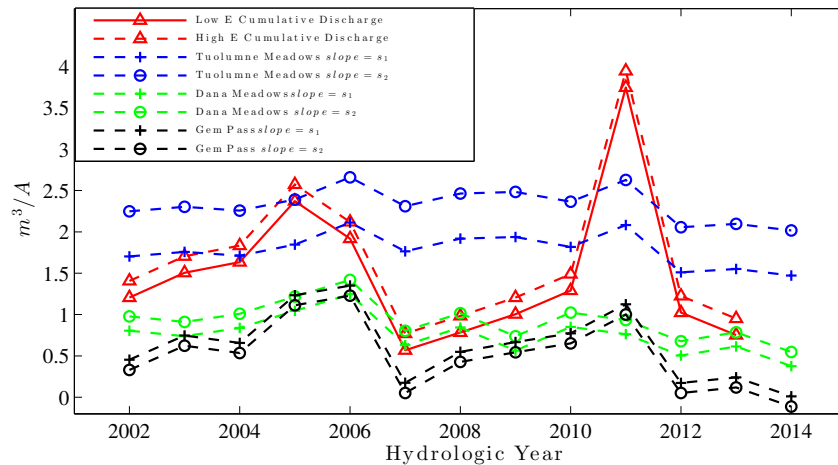


FIGURE 3.14: Tuolumne FATB Precipitation Models and Cumulative Discharge  
Six precipitation models compared to cumulative discharge data at Twin Bridges. Offsets of 0.3m and 0.5m water equivalent evaporative terms have been added to the cumulative discharge set.

- The 2007, 2008, and 2013 years seem best matched with the Dana MET Station-based model slope  $=s_1$ .
- In 2005 the Tuolumne MET Station-based precipitation model with slope  $=s_1$  best fits the discharge data.

However, most of the hydrologic years show no direct coincidence with any precipitation model. 2011 especially shows a much larger deviation than any precipitation model considered. Curiously, The Gem Pass precipitation model mirrors closely the waveform of the discharge data, albeit of a smaller magnitude.

The Lyell Creek BLWC and Maclure Creek Basins show a much better fit with their proposed precipitation models, illustrated in figure 3.15. The Tuolumne MET Station-based models all show much larger than expected precipitation inputs, as does the Dana-Based model with slope  $s_1$ . All other models do seem to follow what would be expected from a glacial basin experiencing a negative or near negative hydrologic basin balance.

### 3.3.3 Precipitation Model Conclusion

Of the precipitation models for the Tuolumne FATB Basin, no single model seems to follow the observed cumulative discharge and expected spread of evaporation for the

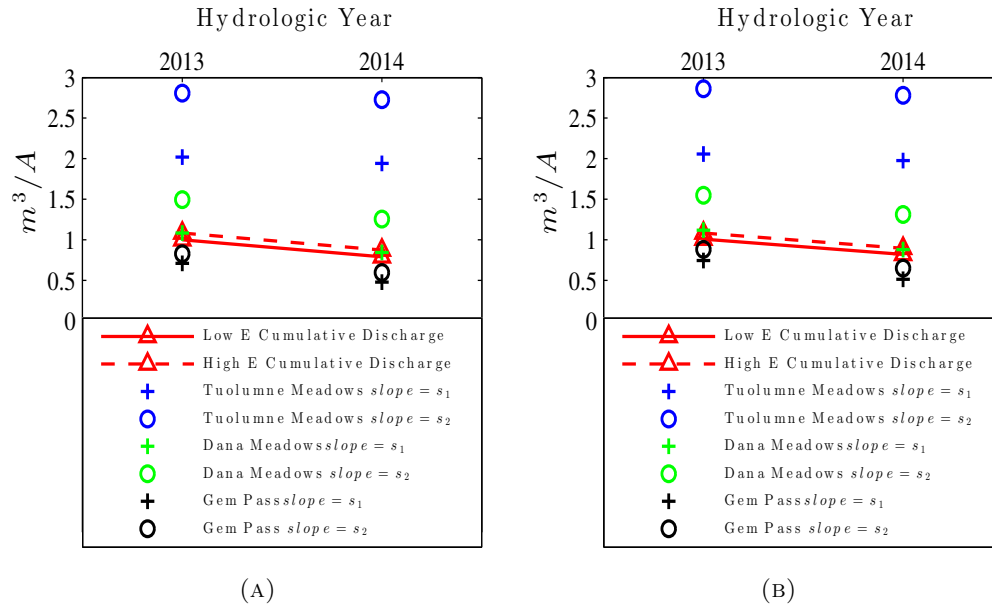


FIGURE 3.15: Lyell BLWC and Maclure Creek Basin Cumulative Discharge and Precipitation

(A) compares precipitation models and discharge plus evaporation estimates for Lyell Creek BLWC Basin. (B) compares precipitation models and discharge plus evaporation estimates for Maclure Creek Basin.  $E_{min}$  and  $E_{max}$  were calculated based on section 2.1.2. Maclure Creek Basin E offset values are  $E_{min} = 0.113\text{m}$  and  $E_{max} = 0.188\text{m}$ ; Lyell Creek BLWC Basin E offset values are  $E_{min} = 0.126\text{m}$  and  $E_{max} = 0.209\text{m}$ .

basin. Several models did seem to plausible for the basin during select years, and the Gem Pass MET Station models did seem to follow the waveform of the discharge.

Since all three precipitation models are samples of conditions taken at a particular altitude and year, it is possible that none of the stations are representative of the precipitation input to the study basins. The true basin water input is more likely to be a linear combination of models, essentially averaging the SWE recorded at each station per year. Linear combinations of models can be made in several ways as outlined below:

$$P_{model} = P_{Di} \quad (3.1)$$

$$P_{model} = \frac{P_{D1} + P_{G2}}{2} \quad (3.2)$$

$$P_{model} = \frac{P_{D1} + P_{D2}}{2} \quad (3.3)$$

$$P_{model} = \frac{P_{D1} + P_{D2} + P_{G2}}{3} \quad (3.4)$$

$$P_{model} = \frac{P_{D1} + P_{T1} + P_{G1}}{3} \quad (3.5)$$

Basin	Signal Amplitude ( $\text{m}^3/A$ )
Tuolumne FATB	0.013
Lyell Creek BLWC	0.085
Maclure Creek	0.075
Lyell Creek ABVC	0.097

TABLE 3.2: Expected Melt Signal Amplitude by Basin  
 Observations from 2002-2014 by the [National Park Service, Unpublished Glacier Data](#) estimate glacial melt to be constrained to +1 to -2.5 vertical meters of SWE per year. Listed above are 1m SWE melt values averaged over the basin area.

$$P_{model} = \frac{P_{D1} + P_{D2} + P_{G1} + P_{G2}}{4} \quad (3.6)$$

28 unique combinations of precipitation models can be made<sup>1 2</sup>(resulting in 56 possible basin balances per year when the two evaporative extremes are considered). The resulting basin balances can either be kept or rejected based on expected balances or all models can be considered.

According to photographic observations and glacier transect surveys [[National Park Service, Unpublished Glacier Data](#)], reasonable  $\Delta M$  values range from 1m (accumulation) to -2.5m (melt) as averaged over the glacier area. Table 3.2 lists the basin-averaged signal magnitude representing 1m vertical glacial melt (in SWE). If only precipitation models which result in basin balances that fall within this range are considered, the data may suffer from sample bias. One way of testing the bias degree is if the cumulative distribution function of the data is similar to a uniform distribution. The [Kolmogorov-Smirnov](#) or KT statistical test determines the likelihood that the data is the result of a given cumulative distribution, and thus can be used to examine the significance of these 'conforming' models.

### 3.4 Basin Balance Analysis

Basin balance analysis consists of two parts: calculation of the absolute differences in water input/output from the system, and calculation of the g constant from section 2.1.5.

<sup>1</sup>3.1 is the simple one slope, one MET Station model. 3.2 is a linear combination of two models, the only requirement that it not reduce down to 3.1. 3.3 is an average of the upper and lower slope models utilizing a single MET Station. 3.4 is the average of three precipitation models that do not reduce down to 3.2. 3.5 is the average precipitation from three separate stations utilizing a single slope. 3.6 is the average of both slope models at two separate stations.

<sup>2</sup>Letter subscripts refer to the station the model is sourced from i.e. D = Dana, T = Tuolumne, G = Gem Pass. Number subscripts refer to the slope model used from 3.11, with 1 = slope of 1.99 meter SWE per km elevation, and 2 = 3.01 meter SWE per km elevation.

Difference in basin water input vs. output is calculated by subtracting cumulative discharge and a selected evaporation model from a particular precipitation model.

Since the basin hydrologic balance is defined as 3.7,  $g_0$  will be calculated based on equation 3.8.

$$P - Q - E = B \quad (3.7)$$

$$B = a_i \cdot T \cdot g_0 \quad (3.8)$$

Where B is defined as the basin water balance. Equations 3.7 and 3.8 will be unique for each precipitation model plus evaporation model used.

### 3.4.1 Lyell Creek Below Confluence Basin Balance Results

For the following two sections, refer to tables 3.3 and 3.4 and boxplots 3.16 and 3.17.

#### 3.4.1.1 All Balance Models

Water balance spreads of Lyell Creek BLWC Basin for hydrologic years 2013 and 2014 were largely positive. Hydrologic year 2013 had a mean positive balance of  $0.45\text{m}^3/A$  with a standard deviation of  $0.43\text{m}^3/A$ . Hydrologic year 2014 had a mean positive balance of  $0.48\text{m}^3/A$  with a standard deviation of  $0.47\text{m}^3/A$ . Both the mean and standard deviation of these basin balance spreads strongly contradict observational evidence by the [National Park Service, Unpublished Glacier Data](#) that suggest these basins were undergoing negative water balances during this time.

The spread of glacial melt constants over this time was also overwhelmingly positive. Hydrologic year 2013 had an average glacial melt constant of  $1.36\text{m SWE}/^\circ\text{C}$  with a standard deviation of  $1.31\text{m SWE}/^\circ\text{C}$ . Hydrologic year 2014 had an average glacial melt constant of  $0.96\text{m SWE}/^\circ\text{C}$  and a standard deviation of  $0.95\text{m SWE}/^\circ\text{C}$ . Positive melt constants indicate decreasing melt with increasing mean summer temperature and are thus likely an artifact of inaccurate SWE input data.

#### 3.4.1.2 Conforming Balance Models

When only balances which followed observational evidence were analyzed, the basin water balances were largely negative. Hydrologic year 2013 exhibited a mean balance of

$-0.023\text{m}^3/A$  with a standard deviation of  $0.109\text{m}^3/A$ . Hydrologic year 2014 exhibited a mean balance of  $-0.034\text{m}^3/A$  with a standard deviation of  $1.086\text{m}^3/A$ .

The spread of glacial melt constants over this time was on average negative. Hydrologic year 2013 had a mean glacial melt constant value of  $-0.094\text{m SWE}/^\circ\text{C}$  with a standard deviation of  $0.3291\text{m SWE}/^\circ\text{C}$ . Hydrologic year 2014 had a mean glacial melt constant value of  $-0.1144\text{m SWE}/^\circ\text{C}$  with a standard deviation of  $0.218\text{m SWE}/^\circ\text{C}$ . Although these melt values are consistent with observed melting rates, it is possible they are an artifact of cherry picking only conforming models.

The p values given by the KT test indicate a  $> 71\%$  chance in 2013 and a  $> 76\%$  in 2014 that these conforming balance values and glacial melt constant values are from a uniform random distribution, making it likely that the data exhibits sampling bias. Even ignoring the results of the KT test, the standard deviations do not preclude positive balances during these years. The Lyell Creek BLWC Basin water balance for the 2013 and 2014 hydrologic years cannot be reasonably calculated by the methods used here.

### 3.4.2 Maclure Creek Basin Balance Results

For the following two sections, refer to tables 3.5 and 3.6 and boxplots 3.18 and 3.19.

#### 3.4.2.1 All Balance Models

Water balance spreads of Maclure Creek Basin for hydrologic years 2013 and 2014 were largely positive. Hydrologic year 2013 had a mean balance of  $0.494\text{m}^3/A$  with a standard deviation of  $0.437\text{m}^3/A$ . Hydrologic year 2014 had a mean balance of  $0.5\text{m}^3/A$  with a standard deviation of  $0.475\text{m}^3/A$ . Both these years strongly contradict observational evidence that Maclure Creek Basin has experienced negative balances during this time.

The spread of glacial melt constants over this time was positive. Hydrologic year 2013 had a mean glacial melt constant of  $1.69\text{m SWE}/^\circ\text{C}$  with a standard deviation of  $1.49\text{m SWE}/^\circ\text{C}$ . Hydrologic year 2014 had a mean glacial melt constant of  $1.15\text{m SWE}/^\circ\text{C}$  with a standard deviation of  $1.089\text{m SWE}/^\circ\text{C}$ . Positive melt constants imply decreasing glacial melt with increasing mean summer temperature and are thus likely an artifact of inaccurate SWE input data.

#### 3.4.2.2 Conforming Balance Models

When only balances which followed observational evidence were analyzed, only hydrologic year 2013 exhibited a partial positive water balance spread. Hydrologic year 2013

had a mean water balance of  $0.0087\text{m}^3/A$  with a standard deviation of  $0.109\text{m}^3/A$ . Hydrologic year 2014 had a basin average of  $-0.375\text{m}^3/A$  with a standard deviation of  $0.108\text{m}^3/A$ .

The spread of glacial melt constants over this time was mostly negative, but the large spread of standard deviations makes these models inconclusive. Hydrologic year 2013 had a mean glacial melt constant of  $0.03\text{m SWE}/^\circ\text{C}$  with a standard deviation of  $0.374\text{m SWE}/^\circ\text{C}$ . Hydrologic year 2014 had a mean glacial melt constant of  $-0.0858\text{m SWE}/^\circ\text{C}$  with a standard deviation of  $0.2478\text{m SWE}/^\circ\text{C}$ .

Although these melt rate constants can be consistent with observational data, the magnitude of the standard deviations is too large to conclusively say this basin had either positive or negative balances during this time. Additionally the KT test indicated a high probability that the basin balances are no different than a uniform distribution between the observational bounds, with a p value of  $> 91\%$  for 2013 and  $> 93\%$  for 2014. The Maclure Creek Basin water balance for these two years therefore cannot be reasonably estimated by the methods used here.

### 3.4.3 Lyell Creek Above Confluence Balance Results

Lyell Creek ABVC Basin models were calculated by subtracting Maclure Creek Basin balance models from their Lyell BLWC Basin model counterparts. refer to tables 3.7 and 3.8 and boxplots 3.20 and 3.21 for the following section.

#### 3.4.3.1 All Balance Models

Water balances of Maclure Creek Basin for hydrologic years 2013 and 2014 were largely positive, although the size of the standard deviation did not preclude negative balances. Hydrologic Year 2013 had a mean water balance of  $0.4131\text{m}^3/A$  and a standard deviation of  $0.4348\text{m}^3/A$ . Hydrologic Year 2014 had a mean water balance of  $0.46\text{m}^3/A$  and a standard deviation of  $0.4728\text{m}^3/A$ . These largely positive model spreads contradict observational evidence that the Lyell Creek ABVC Basin should have negative water balances.

The spread of glacial melt constants over this time was positive. Hydrologic year 2013 had a mean glacial melt constant of  $1.106\text{m SWE}/^\circ\text{C}$  with a standard deviation of  $1.16\text{m SWE}/^\circ\text{C}$ . Hydrologic year 2014 had a mean glacial melt constant of  $0.824\text{m SWE}/^\circ\text{C}$  with a standard deviation of  $0.845\text{m SWE}/^\circ\text{C}$ . Positive melt constants imply decreasing glacial melt with increasing mean summer temperature and are thus likely an artifact of inaccurate SWE input data.

### 3.4.3.2 Conforming Balance Models

When only balances which followed observational evidence were analyzed, both 2013 and 2014 hydrologic years exhibited similar negative basin water balances. Hydrologic year 2013 had a mean water balance of  $-0.0719\text{m}^3/A$  with a standard deviation of  $0.1104\text{m}^3/A$ . Hydrologic year 2014 had a mean water balance of  $-0.0766\text{m}^3/A$  with a standard deviation of  $0.1095\text{m}^3/A$ . This is consistent with observational evidence of negative basin balances.

The standard deviation gives the impression that the basin balance is not as strongly negative as would be expected from a glacial basin undergoing strong net melting. However, a look at boxplot 3.20 and table 3.11 shows that the interquartile range is heavily skewed towards a negative balance: the middle 50% of models for 2013 lie between 0.0077 and  $-0.1454\text{m}^3/A$ ; the middle 50% of models for 2014 lie between 0.0028 and  $-0.1496\text{m}^3/A$ .

The spread of glacial melt constants over this time was mostly negative. Hydrologic year 2013 had a mean glacial melt constant of  $-0.1923\text{m SWE}/^\circ\text{C}$  with a standard deviation of 0.2954m. Hydrologic year 2014 had a mean glacial melt constant of  $-0.1370\text{m SWE}/^\circ\text{C}$  with a standard deviation of 0.1958.

The standard deviation of the melt value gives the impression that the calculated glacial melt constant may be negative. However, the Q1 and Q3 quartile values (boxplot 3.8) show the middle 50% of values between 0.0205 and  $-0.3891\text{m SWE}/^\circ\text{C}$  for 2013, and 0.005 to  $-0.2676\text{m SWE}/^\circ\text{C}$  for 2014. This is expected from a glacial melt constant representative of physical processes within the basin.

Note that these values are lower than the value given in Paterson and Cuffey [2010a] of  $C_T$  (refer to equation 2.5) of  $\approx 1\text{ m SWE}/^\circ\text{C}$ . Explanations for this discrepancy include changes in permanent ice area ( $a_i$ ) since publication of the National Park Service, or an effective adiabatic lapse rate higher than the  $5^\circ\text{C km}^{-1}$  used to calculate the glacial melt constant.

The KT test shows a 33.7% probability in 2013 and 37.3% probability in 2014 that the data follows from a uniform random distribution. While not sufficient to reject this null hypothesis, this test is compelling given that Lyell BLWC Basin's p-value was  $> 70\%$  and Maclure had a  $> 90\%$  p-value. To obtain smaller p-values, a more representative basin analysis will have to be conducted.

Assuming that these data are representative of real basin balances, it is clear that Lyell Creek ABVC Basin has been experiencing net negative water balances for 2013 and 2014. Judging by the positioning of the quartile ranges as seen in boxplot 3.20, and the

area of Lyell Creek ABVC (Maclure Creek Basin - Lyell Creek BLWC Basin in figure 2.2), Lyell Creek ABVC Basin have been undergoing a net water loss of between from 0 to  $1.14 \times 10^6 \text{ m}^3 \text{ yr}^{-1}$ , with an average melt of  $0.55 \times 10^6 \text{ m}^3 \text{ yr}^{-1}$ . The mean value is equivalent to  $\approx 1/2$  the Empire State building's volume worth of water [Wolfram Alpha]. Curiously, this value increased between 2013 and 2014 by  $35 \times 10^3 \text{ m}^3$ , while the glacial melt constant has decreased by 28% during this time. This could indicate that the Lyell Creek ABVC Basin has reached a point where increases in temperature have only a minimal impact on melting as the inventory of glacial ice begins to reduce. It is also possible that changes in glacial ice albedo discovered during the 2014 YNP RMS research expedition affected glacial sensitivity to temperature change. Regardless, the amplitude of this increase is well below the sensitivity limit of this analysis.

These numbers should only be interpreted insofar as the KT test affirms their validity; these values have roughly a third chance of arising purely from random chance. To definitively quantify the glacial melt of this basin, water balance models which are more representative of basin hydrologic fluxes will have to be developed.

### 3.4.4 Tuolumne Fork Above Twin Bridges Basin Balance

For the following sections, refer to tables 3.9 and 3.10 as well as boxplots 3.22 and 3.23.

#### 3.4.4.1 All Balance Models

Water balance models of the Tuolumne FATB Basin for all study years except 2007, 2008, 2009, and 2013 were distributed to the net negative balance end. This may be in part because of the inclusion of Gem Pass MET Station in the models; it lies east of the Sierra Nevada crest and likely records lower precipitation than is in Tuolumne FATB Basin due to the rainshadow effect.

Hydrologic years 2007, 2008, 2009, and 2013 show some positive basin balance spreads, likely because models incorporating Gem Pass MET Station data had much greater interannual variability (see figure 3.14).

Hydrologic year 2011 is anomalously low, with an average basin water balance 2 meters (in  $\text{m}^3/\text{A}$ ) lower than all other years. This large negative balance indicates that none of the precipitation models considered accurately represents the precipitation during this time period.

The glacial melt constants for this basin follow trends in the balances; 2007-09 and 2013 all show positive glacial melt constants (paradoxically decreasing melt from increasing

summer temperature). 2011's glacial melt constant of  $-38 \text{ m SWE}/^\circ\text{C}$  deviates enough from the observed values that this year will no longer be considered in the analysis. The spread of melt constants is also quite high ( $> 4.6$ ) compared to those found in the Lyell Creek BLWC ( $< 1.4$ ), Maclure Creek ( $< 1.5$ ), and Lyell Creek ABVC ( $< 1.2$ ) analysis of all models.

#### 3.4.4.2 Conforming Balance Models

Conforming water balance models show means of at or below zero for all years. Hydrologic year 2004 shows the lowest average basin balance of  $-0.0807 \text{ m}^3/\text{A}$  with standard deviation  $0.1414\text{m}^3/\text{A}$ . 2007 has the highest average basin balance with  $0.0014 \text{ m}^3/\text{A}$  with a standard deviation of  $0.1162\text{m}^3/\text{A}$ .

Derived conforming glacial melt constants also show values at or below zero for all years. Hydrologic year 2008 has the lowest mean melt constant of  $-0.481 \text{ m SWE}/^\circ\text{C}$  with a standard deviation of  $1.753\text{m SWE}/^\circ\text{C}$ . 2007 has the highest mean melt constant of  $0.0184\text{m SWE}/^\circ\text{C}$  with a standard deviation of  $1.553\text{m SWE}/^\circ\text{C}$ .

The KT test for these data show that excepting 2005 and 2009, all conforming model spreads have a greater than  $> 76\%$  chance of arising from a uniform random distribution. Hydrologic years 2005 and 2009 have probabilities of 50% and 44% respectively; not enough to reject the null hypothesis, but as these probabilities are lower than all other data it is worth noting their calculated basin balances. Hydrologic year 2005 conforming models had a mean basin balance of  $-0.0807\text{m}^3/\text{A}$  with a standard deviation of  $0.1414\text{m}$ . Hydrologic year 2009 had a mean basin balance of  $-0.0233\text{m}^3/\text{A}$  with a standard deviation of  $0.1158\text{m}$ , although the conforming models were spread out more below the mean than above it based on boxplot 3.22.

Mean values are a factor of 8 (2005) to 2 (2009) larger than the expected melt signal amplitude. 2005 is especially troubling as only two of the possible 24 models were considered (hence the lack of whiskers in boxplot 3.22. Both of the standard deviations for these two years are approximately half the estimated evaporation range of  $0.3\text{-}0.5\text{m}^3/\text{A}$  for the basin, indicating that the precision of the conforming models during 2009 are limited by the precision of the evaporation models used.

Based on the p-values, lack of accurate precipitation models, and precision of evaporation bounds, this analysis of the Lyell fork of the Tuolumne River Basin Above Twin Bridges is of limited use. Only the mean water loss volume during 2009 of  $2.4 \times 10^6\text{m}^3$  is of interest with its relatively low p-value of 44%, but this number is of limited use considering the standard deviation is an order of magnitude higher than this value. Future studies will need to incorporate more representative precipitation and evaporation models.

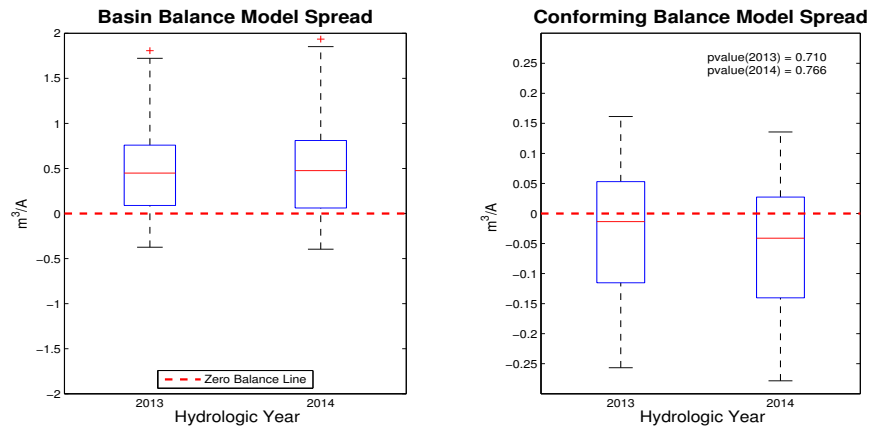


FIGURE 3.16: Lyell Creek BLWC Basin Water Balance  
 Lyell Creek BLWC Basin water balance model distribution. Left plot is the spread of all models. Right plot shows the distribution of conforming models that fall within observational bounds. Dotted line indicates the zero balance reference; the point at which basin water inputs equal all basin water outputs. Mean and standard deviation values can be found in 3.3.

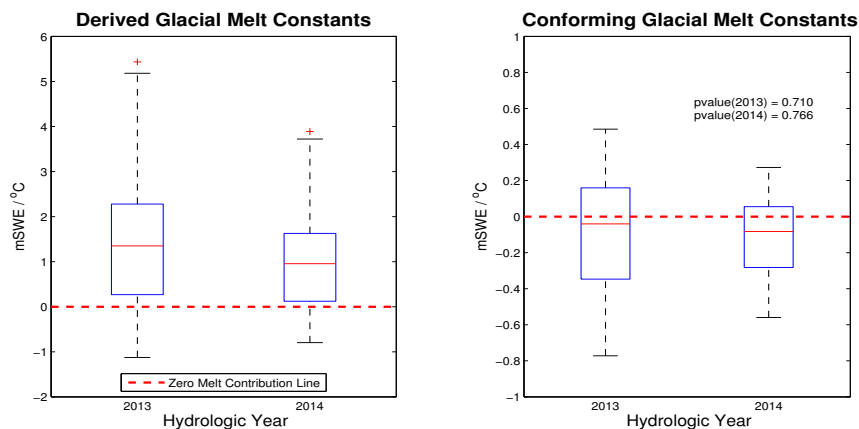


FIGURE 3.17: Lyell Creek Basin BLWC Glacial Melt Constants  
 Lyell Creek BLWC Basin glacial melt constants distribution. Left plot is the spread of the melt constants calculated by 3.8 from all models. Right plot shows the distribution of conforming glacial melt constants from models within observational bounds. Dotted line indicates the zero melt contribution reference; values above this line imply increased melt with decreasing average summer temperature. Mean and standard deviation values can be found in 3.4.

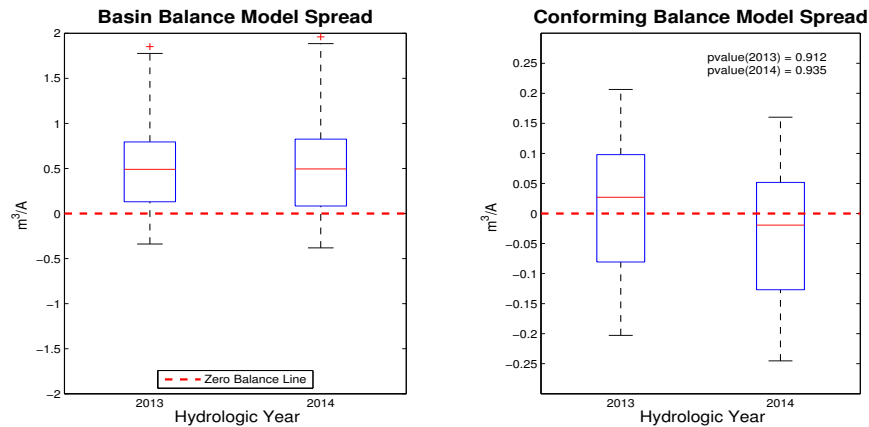


FIGURE 3.18: Maclure Creek Basin Water Balance

Maclure Creek Basin water balance model distribution. Left plot is the spread of all models. Right plot shows the distribution of conforming models that fall within observational bounds. Dotted line indicates the zero balance reference; the point at which basin water inputs equal all basin water outputs. Mean and standard deviation values can be found in 3.5.

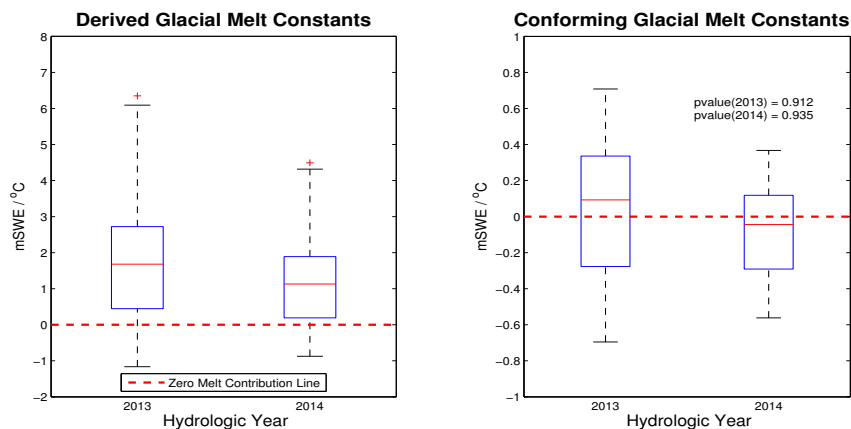


FIGURE 3.19: Maclure Creek Basin Glacial Melt Constants

Maclure Creek Basin glacial melt constants distribution. Left plot is the spread of the melt constants calculated by 3.8 from all models. Right plot shows the distribution of conforming glacial melt constants from models within observational bounds. Dotted line indicates the zero melt contribution reference; values above this line imply increased melt with decreasing average summer temperature. Mean and standard deviation values can be found in 3.6.

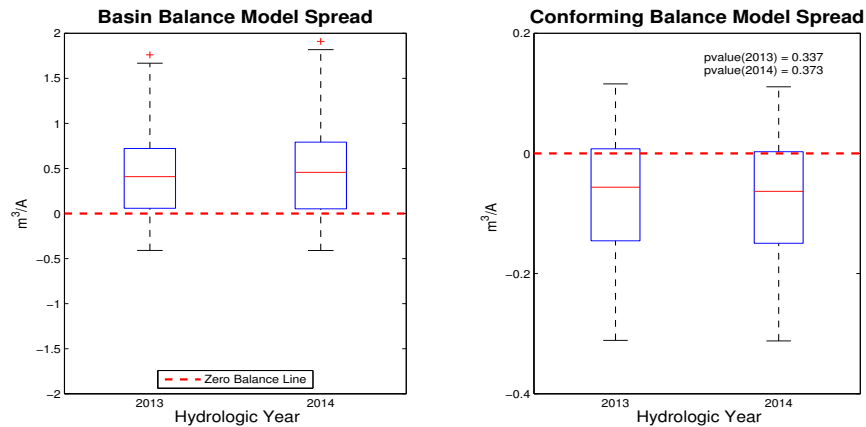


FIGURE 3.20: Lyell Creek ABVC Basin Water Balance  
 Lyell Creek ABVC Basin water balance model distribution. Left plot is the spread of all models. Right plot shows the distribution of conforming models that fall within observational bounds. Dotted line indicates the zero balance reference; the point at which basin water inputs equal all basin water outputs. Mean and standard deviation values can be found in 3.7.

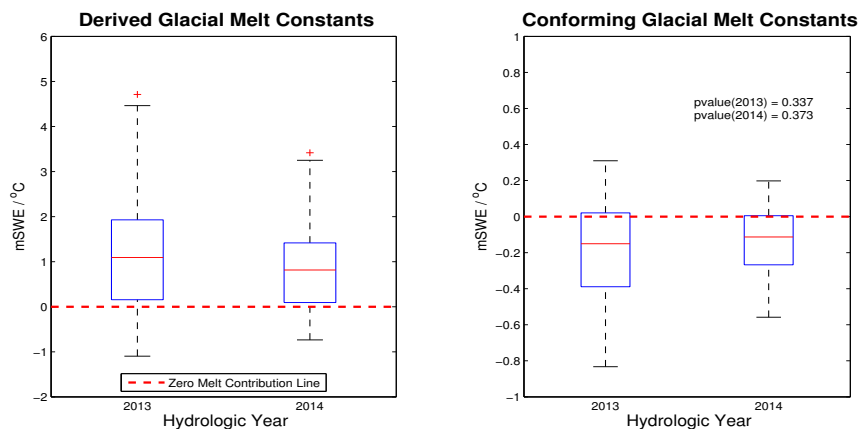


FIGURE 3.21: Lyell Creek ABVC Basin Glacial Melt Constants  
 Lyell Creek ABVC Basin glacial melt constants distribution. Left plot is the spread of the melt constants calculated by 3.8 from all models. Right plot shows the distribution of conforming glacial melt constants from models within observational bounds. Dotted line indicates the zero melt contribution reference; values above this line imply increased melt with decreasing average summer temperature. Mean and standard deviation values can be found in 3.8.

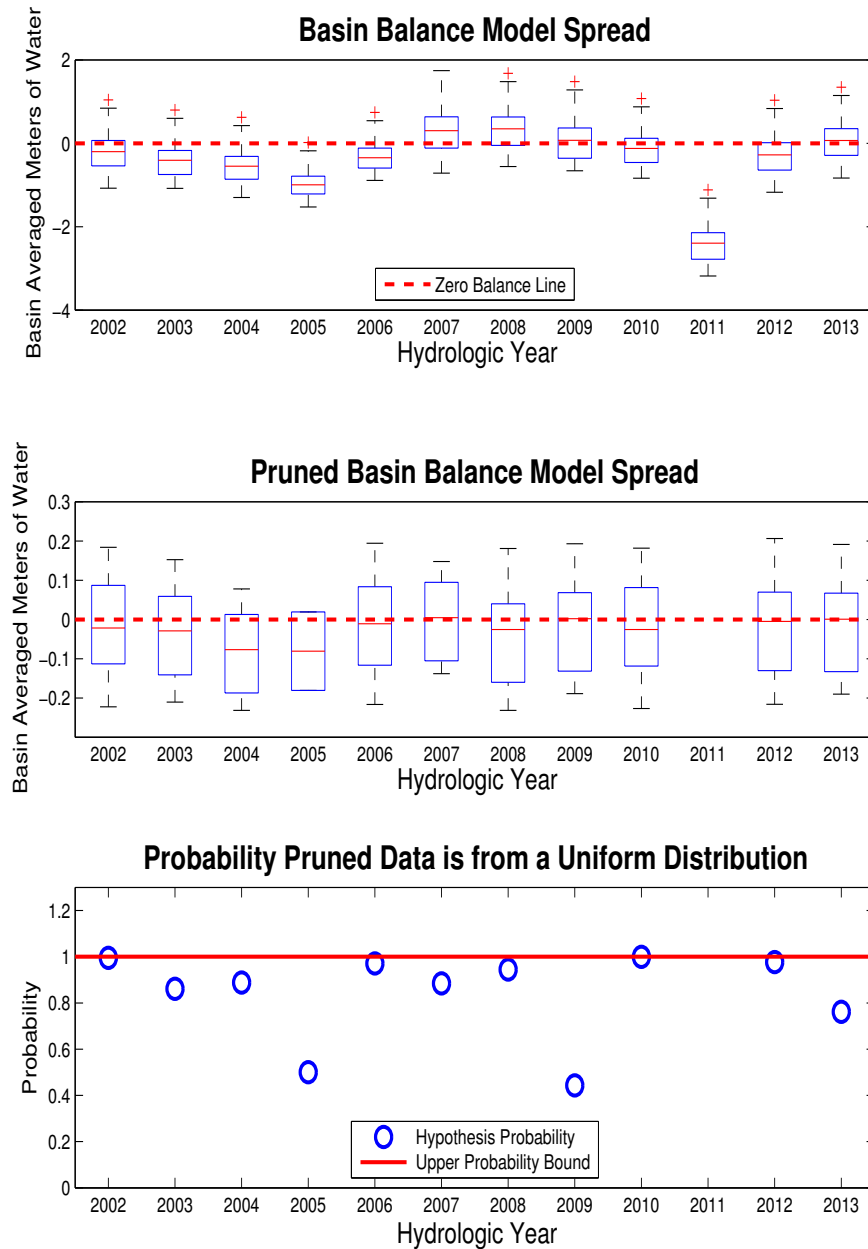


FIGURE 3.22: Tuolumne Fork Above Twin Bridges Basin Water Balance  
 Tuolumne FATB Basin water balance model distribution. Left plot is the spread of all models. Right plot shows the distribution of conforming models that fall within observational bounds. Dotted line indicates the zero balance reference; the point at which basin water inputs equal all basin water outputs. Solid line is the reference line for the KT test; at the line there is a 100% chance that conforming models on that year arise from a uniform random distribution. Note that no conforming models nor KT test exist for 2011 as all water balance models for that hydrologic year exceeded observational bounds. Mean and standard deviation values can be found in 3.9.

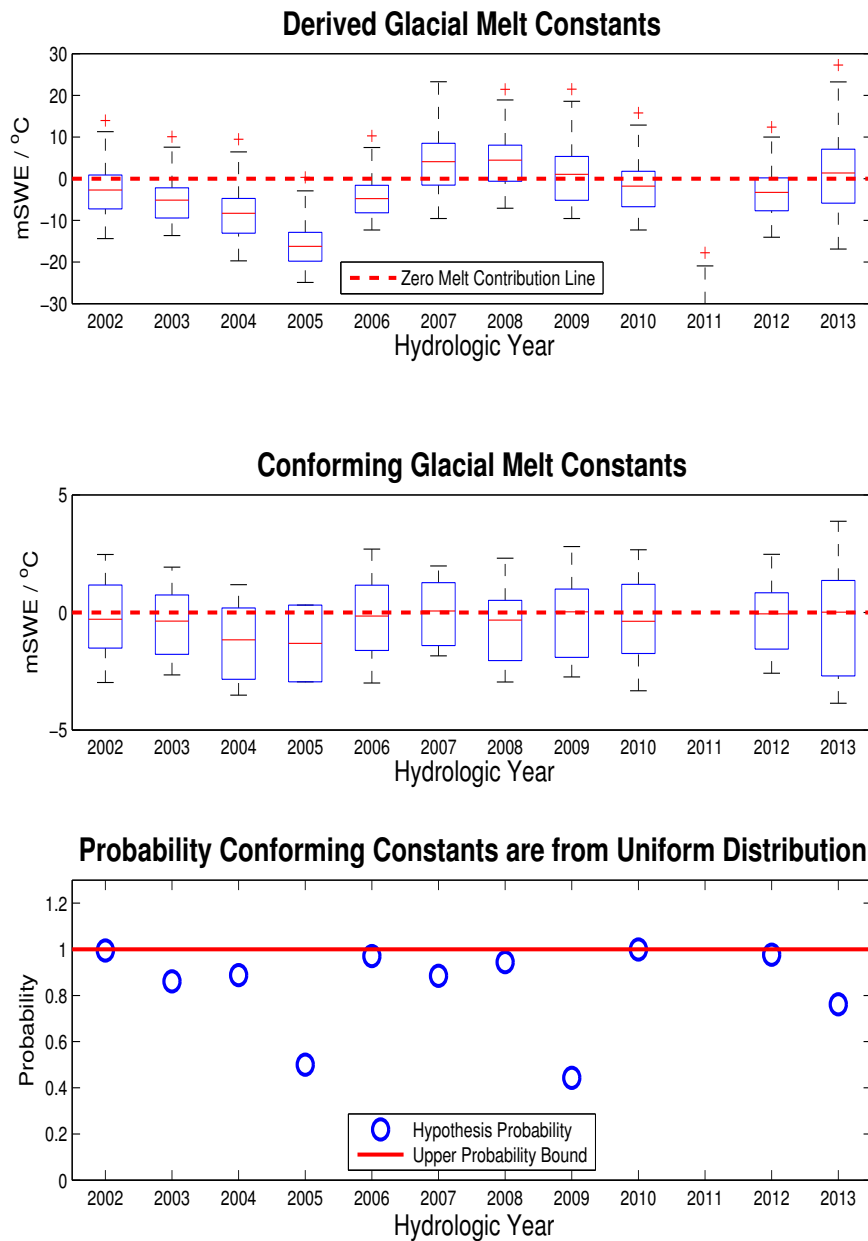


FIGURE 3.23: Tuolumne Fork Above Twin Bridges Basin Glacial Melt Constants  
 Tuolumne FATB Basin glacial melt constants distribution. Left plot is the spread of the melt constants calculated by 3.8 from all models. Right plot shows the distribution of conforming glacial melt constants from models within observational bounds. Dotted line indicates the zero melt contribution reference; values above this line imply increased melt with decreasing average summer temperature. Solid line is the reference line for the KT test; at the line there is a 100% chance that conforming models on that year arise from a uniform random distribution. Note that no conforming glacial constants nor KT test exist for 2011 as all water balance models for that hydrologic year exceeded observational bounds. Mean and standard deviation values can be found in 3.10.

Hydrologic Year	All Models				Conforming Models				Null Hypothesis p value
	m <sup>3</sup> /A		Volume m <sup>3</sup> × 10 <sup>4</sup> m <sup>3</sup>		m <sup>3</sup> /A		Volume m <sup>3</sup> × 10 <sup>4</sup> m <sup>3</sup>		
	Mean	StDev	Mean	StDev	Mean	StDev	Mean	StDev	
2013	0.4539	0.4359	693.8	666.4	-0.0234	0.1094	-47.95	187.4	0.7104
2014	0.4806	0.4739	734.7	724.3	-0.0346	0.1086	-87.04	174.9	0.7660

TABLE 3.3: Calculated Basin Water Balance for Lyell Creek BLWC Basin

Lyell Creek BLWC basin water balance was calculated according to 3.7 and by using water input models outlined in section 3.3.3. Shown are both the basin-averaged meters of water values and the water volumes in  $m^3 \times 10^4$ . Both values from the set of all models and the set of conforming models are listed. KT test values represent the likelihood that the pruned model spread arises from a uniform random distribution. Above model data correspond to boxplot 3.16.

Hydrologic Year	All Models		Pruned Models		Null Hypothesis p Value
	Mean	StDev	Mean	StDev	
2013	1.365	1.311	-0.0944	0.3291	0.7104
2014	0.966	0.9525	-0.1144	0.2182	0.7660

TABLE 3.4: Calculated Glacial Melt Constants for Lyell Creek BLWC Basin

Glacial melt constants for Lyell Creek BLWC basin were calculated from equation 3.7 and are in units of m SWE/°C. Shown are values calculated for all models as well as only models which fell within observational bounds. P values from the KT test are identical to the corresponding basin balance KT test contained in table 3.3. Above model data correspond to boxplot 3.17.

Hydrologic Year	All Models				Conforming Models				Null Hypothesis p value
	m <sup>3</sup> /A		Volume m <sup>3</sup> × 10 <sup>4</sup> m <sup>3</sup>		m <sup>3</sup> /A		Volume m <sup>3</sup> × 10 <sup>4</sup> m <sup>3</sup>		
	Mean	StDev	Mean	StDev	Mean	StDev	Mean	StDev	
2013	0.4942	0.4372	379.7	335.9	0.0087	0.1089	6.691	83.69	0.9121
2014	0.5003	0.4750	384.4	365.0	-0.0375	0.1081	-28.78	83.08	0.9346

TABLE 3.5: Calculated Basin Water Balance for Maclure Creek Basin

Maclure Creek basin water balance was calculated according to 3.7 and by using water input models outlined in section 3.3.3. Shown are both m<sup>3</sup>/A values and water volumes in  $m^3 \times 10^4 m^3$ . Both values from the set of all models and the set of conforming models are listed. KT test values represent the likelihood that the pruned model spread arises from a uniform random distribution. Above model data correspond to boxplot 3.18.

Hydrologic Year	All Models		Conforming Models		Null Hypothesis p Value
	Mean	StDev	Mean	StDev	
2013	1.695	1.499	0.0299	0.3735	0.7104
2014	1.146	1.089	-0.0858	0.2478	0.7660

TABLE 3.6: Calculated Glacial Melt Constants for Maclure Creek Basin  
 Glacial melt constants for Maclure Creek basin were calculated from equation 3.7 and are in units of m SWE/ $^{\circ}$ C. Shown are values calculated for all models as well as only models which fell within observational bounds. P values from the KT test are identical to the corresponding basin balance KT test contained in table 3.5. Above model data correspond to boxplot 3.19.

Hydrologic Year	All Models				Conforming Models				Null Hypothesis p value
	$m^3/A$		Volume $m^3 \times 10^4 m^3$		$m^3/A$		Volume $m^3 \times 10^4 m^3$		
	Mean	StDev	Mean	StDev	Mean	StDev	Mean	StDev	
2013	0.4131	0.4348	314.1	330.5	-0.0719	0.1104	-54.64	83.93	0.3368
2014	0.4607	0.4728	350.25	359.4	-0.0766	0.1095	-58.26	83.26	0.3727

TABLE 3.7: Calculated Basin Water Balance for Lyell Creek ABVC Basin  
 Lyell Creek ABVC basin water balance was calculated according to 3.7 and by using water input models outlined in section 3.3.3. Shown are both  $m^3/A$  values and water volumes in  $m^3 \times 10^4 m^3$ . Both values from the set of all models and the set of conforming models are listed. KT test values represent the likelihood that the conforming model spread arises from a uniform random distribution. Above model data correspond to boxplot 3.20.

Hydrologic Year	All Models		Conforming Models		Null Hypothesis p Value
	Mean	StDev	Mean	StDev	
2013	1.106	1.1635	-0.1923	0.2954	0.3368
2014	0.8239	0.8455	-0.1370	0.1958	0.3727

TABLE 3.8: Calculated Glacial Melt Constants for Lyell Creek ABVC Basin  
 Glacial melt constants for Lyell Creek ABVC basin were calculated from equation 3.7 and are in units of m SWE/ $^{\circ}$ C. Shown are values calculated for all models as well as only models which fell within observational bounds. P values from the KT test are identical to the corresponding basin balance KT test contained in table 3.7. Above model data correspond to boxplot 3.21.

Hydrologic Year	All Models				Conforming Models				Null Hypothesis p value
	m <sup>3</sup> /A		Volume m <sup>3</sup> × 10 <sup>4</sup> m <sup>3</sup>		m <sup>3</sup> /A		Volume m <sup>3</sup> × 10 <sup>4</sup> m <sup>3</sup>		
	Mean	StDev	Mean	StDev	Mean	StDev	Mean	StDev	
2002	-0.2147	0.4156	-2340	4531	-0.0234	0.1226	-254.7	1336	0.9952
2003	-0.4188	0.3829	-4566	4175	-0.0346	0.1144	-377.7	1247	0.8612
2004	-0.5606	0.3773	-6122	4113	-0.0821	0.1152	-895.4	1256	0.8882
2005	-0.9933	0.303	-10830	3303	-0.0807	0.1414	-879.8	1542	0.5000
2006	-0.3443	0.3300	-3753	3598	-0.0159	0.1163	-173.1	1268	0.9709
2007	0.2936	0.4959	3201	5407	0.0014	0.1162	14.98	1267	0.8849
2008	0.3253	0.4489	3547	4894	-0.0377	0.1320	-410.5	1438	0.9445
2009	0.0592	0.4613	645.5	5029	-0.0233	0.1158	-242.6	1263	0.4433
2010	-0.1371	0.3832	-1494	4178	-0.0299	0.1193	-325.5	1301	0.9993
2011	-2.41	0.4157	-26340	4531	–	–	–	–	–
2012	-0.2894	0.4157	-26350	4531	-0.0103	0.1233	-122.5	1344	0.9765
2013	0.0552	0.4299	601.5	4686	-0.0149	0.1141	-162.5	1244	0.7618

TABLE 3.9: Calculated Basin Water Balance for Tuolumne Basin Above Twin Bridges  
 Tuolumne FATB basin water balance was calculated according to 3.7 and by using water input models outlined in section 3.3.3. Shown are both m<sup>3</sup>/A values and water volumes in m<sup>3</sup> × 10<sup>4</sup>m<sup>3</sup>. Both values from the set of all models and the set of conforming models are listed. KT test values represent the likelihood that the pruned model spread arises from a uniform random distribution. Note that no pruned values exist for 2011 because no models fell within expected observational bounds. Above model data correspond to boxplot 3.22.

Hydrologic Year	All Models		Conforming Models		Null Hypothesis p Value
	Mean	StDev	Mean	StDev	
2002	-2.875	5.566	-0.3129	1.642	0.9952
2003	-5.287	4.834	-0.4374	1.444	0.8612
2004	-8.511	5.729	-1.247	1.749	0.8882
2005	-16.21	4.946	-1.317	2.309	0.5000
2006	-4.771	4.574	-0.2200	1.612	0.9709
2007	3.922	6.626	0.0184	1.553	0.8849
2008	4.156	5.735	-0.4810	1.686	0.9445
2009	0.8594	6.696	-0.3230	1.681	0.4433
2010	-2.013	5.629	-0.4386	1.753	0.9993
2011	-38.42	6.609	–	–	–
2012	-3.464	5.255	-0.1236	1.476	0.9765
2013	1.119	8.718	-0.3024	2.313	0.7618

TABLE 3.10: Calculated Glacial Melt Constants for Tuolumne Basin Above Twin Bridges

Glacial melt constants for Tuolumne FATB basin were calculated from equation 3.7 and are in units of m SWE/°C. Shown are values calculated for all models as well as only models which fell within observational bounds. P values from the KT test are identical to the corresponding basin balance KT test contained in table 3.9. Note that no conforming model melt constant data are available for 2011 as all water balance models fell outside the observational bounds. Above model data correspond to boxplot 3.23.

Basin and Hydrologic Year	Q1		Q3		IQR	
	$\text{m}^3/A$	Volume $1 \times 10^3 \text{m}^3$	$\text{m}^3/A$	Volume $1 \times 10^3 \text{m}^3$	$\text{m}^3/A$	Volume $1 \times 10^3 \text{m}^3$
Tuolumne FATB 2009	-0.1316	-14,350	0.0684	7,454	0.2000	21,804
Lyell ABVC 2013	-0.1454	-1,105	0.0077	58.2	0.1531	1,164
Lyell ABVC 2014	-0.1496	-1,137	0.0028	21.4	0.1524	1,159

TABLE 3.11: Selected Basin and Year Water Balance Quantile Statistics  
 Selected interquartile statistics for three basin water balance spreads with lowest KT test statistic. Values are in  $\text{m}^3/A$  of water and  $1 \times 10^3 \text{m}^3$  water. Column Q1 lists values of the first quartile and Q3 lists values of the third quartile. 50% of conforming model values fall between Q1 and Q3.

Basin and Hydrologic Year	Q1	Q3	IQR
Tuolumne FATB 2009	-1.910	0.992	0.918
Lyell ABVC 2013	-0.3891	0.0205	0.4096
Lyell ABVC 2014	-0.2676	0.0050	0.2726

TABLE 3.12: Basin and Year Glacial Melt Constant Quantile Statistics  
 Selected interquartile statistics for three glacial melt constant (as calculated by equation 3.8) spreads with lowest KT test statistic. All values are in  $\text{m SWE}/^\circ\text{C}$ . Column Q1 lists values of the first quartile and  $Q_3$  lists values of the third quartile. 50% of conforming model values fall between Q1 and Q3.

## Chapter 4

# Conclusion

A total of 56 unique basin water balance models for each hydrologic year were calculated from linear combinations of snow pillow data, evapotranspiration limits, and cumulative discharge data. Water balance models that produced net balances that were inconsistent with observations by the [National Park Service, Unpublished Glacier Data](#) were not considered. Remaining balance models were evaluated by a [Kolmogorov-Smirnov](#) statistical test to quantify how susceptible the remaining models were to sampling bias.

All model spreads were determined to be statistically insignificant ( $p > 0.05$ ) from a uniform distribution between the observed melt bounds. However three conforming model spreads exhibited lower  $p$  values ( $p < 0.5$ ) relative to the rest of the model spreads ( $p > 0.71$ ): Tuolumne river above twin bridges water balance in 2009 and derived water balance of Lyell creek above confluence with Maclure creek in 2013 and 2014. It was found that although all three were consistent with observations by [Tangborn \[1977\]](#), [Dean \[1974\]](#) and [Basagic and Fountain \[2011\]](#), the evapotranspiration and precipitation models used did not quantify net glacial loss better than other studies done on these glaciers.

### 4.1 Water Balance at Tuolumne River Above Twin Bridges

For the 2009 hydrologic year, conforming water balance models on the Tuolumne River above Twin Bridges exhibited a mean net water balance of  $-0.0299\text{m}^3/A$  with a standard deviation of  $0.1193\text{m}^3/A$ . The middle 50% of conforming models fell between  $-0.1316$  and  $0.0064\text{m}^3/A$ . Observational evidence by the [National Park Service, Unpublished Glacier Data](#) predicted a glacial melt signal on the order of  $0.013\text{m}^3/A$ ; both the interquartile range and standard deviation are too large to verify this assumption. The KT value for

this model set and hydrologic year was also quite high ( $p = 0.4433$ ), giving this basin analysis a roughly 1 in 2 chance that the results are not statistically different than a uniform random variable picked within observational bounds.

## 4.2 Water Balance at Lyell Creek Above Confluence with Maclure Creek

For the 2013 hydrologic year, conforming water balance model spreads on Lyell Creek Above confluence had a mean net basin balance of  $-0.0719\text{m}^3/A$  with a standard deviation of  $0.1104\text{m}^3/A$ . The middle 50% of conforming models fell between  $-0.1454$  and  $0.0077\text{m}^3/A$ . This represents a basin volume balance between  $+58.2 \times 10^3\text{m}^3/A$  and  $-1,105 \times 10^3\text{m}^3/A$  water. The expected signal from 1m SWE of glacial melt averaged over the glacier (see figure 3.2) is  $0.097\text{m}^3/A$ , ( $-0.74 \times 10^3\text{m}^3$  water), near the lower end of the interquartile range of conforming model spreads. Conforming models for the 2013 hydrologic year exhibited a  $p$  value of 0.3368, giving this analysis a roughly 1 in 3 chance that the results are not statistically different than a uniform random variable picked within observational bounds.

For the 2014 hydrologic year, conforming water balance model spreads on Lyell Creek Above confluence had a mean net basin balance of  $-0.0766\text{m}^3/A$  with a standard deviation of  $0.1095\text{m}^3/A$ . The middle 50% of conforming models fell between  $-0.1496$  and  $0.0028\text{m}^3/A$ . This represents a basin balance between  $+21.4 \times 10^3\text{m}^3$  and  $-1,159 \times 10^3\text{m}^3$  water. The expected signal from 1m SWE of glacial melt fell near the lower end of the interquartile range of conforming model spreads. Conforming models for the 2013 hydrologic year exhibited a  $p$  value of 0.3727, giving this analysis a roughly 1 in 3 chance that the results are not statistically different than a uniform random variable picked within observational bounds.

Sensitivities of glacial melt to mean annual temperature were also examined through the approximation that glacial melt is proportional to mean annual temperature [Paterson and Cuffey, 2010a]:

$$B = A_i \times g \times T \quad (4.1)$$

Where  $B$  is basin water balance in units of  $\text{m}^3$ ,  $A_i$  is glacier area in units of  $\text{m}^2$ ,  $T$  is mean summer temperature at the glacier in units of  $^\circ\text{C}$ , and  $g$  is the glacial melt constant in units of  $\text{m SWE} / ^\circ\text{C}$ . For 2013, the glacial melt constant was observed to have a mean of  $-0.1923\text{m SWE} / ^\circ\text{C}$  with a standard deviation of  $0.2954\text{m SWE} / ^\circ\text{C}$ . The glacial melt constant for 2014 had a mean of  $-0.1370\text{m SWE} / ^\circ\text{C}$  with a standard deviation of  $0.1958\text{m SWE} / ^\circ\text{C}$ . The standard deviations obscure the degree

of weighting of model spreads towards the lower melt constant values. A look at the first and third quartile values for 2013 shows a much larger negative bias than would be expected. First quartile value for 2013 is  $-0.3891\text{m SWE} / ^\circ\text{C}$  and third quartile is  $-0.205\text{m SWE} / ^\circ\text{C}$ . First quartile value for 2014 is  $-0.2676\text{m SWE} / ^\circ\text{C}$  and third quartile is  $0.0050\text{m SWE} / ^\circ\text{C}$ .

If the mean melt constant values are representative of the actual melt constant values, then it can be inferred that Lyell Glacier had a weaker melt response (28% smaller  $g$  constant) to increased mean summer temperatures in 2014 than in 2013. This melt response reduction can be accomplished by a corresponding reduction in glacial surface area or a change in energy coupling to the atmosphere. A research expedition in September 2014 did find bedrock protruding through the middle of Lyell Glacier not present in 2013, signaling a potential change in ambient air heat transfer. However, neither the change in albedo or nor glacial area was monitored over the course of the study period. Additionally both the standard deviations and  $p$  values preclude such analysis from being conclusive.

### 4.3 Comparison With Similar Studies

[Tangborn \[1977\]](#) found that for the 1967 hydrologic year Maclure Glacier lost an average of  $-0.06\text{m}$  of water averaged over the glacier area. This corresponds to a water volume loss of  $-10.2 \times 10^3\text{m}^3 \pm 200\text{m}^3$ .

[Dean \[1974\]](#) examined the water balance for Maclure Glacier from 1967-1972 and found a slight gain of  $0.11\text{m}$  water averaged over the study period. Individual years varied as much as  $+1.21\text{m}$  to as little as  $-0.77\text{m}$  of accumulation/loss over the glacier area. This corresponds to a mean volume gain of  $-21 \times 10^3\text{m}^3$ , a maximum water balance of  $378 \times 10^3\text{m}^3$ , and a minimum water balance of  $-262 \times 10^3\text{m}^3$ .

[Basagic and Fountain \[2011\]](#) performed area-volume scaling studies including the Lyell and Maclure Glaciers. Based on empirical constants provided by [Bahr \[1997\]](#), Lyell Glacier has lost  $136 \times 10^3\text{m}^3 \pm 68 \times 10^3\text{m}^3$  of water per year and Maclure Glacier has lost  $19 \times 10^3\text{m}^3 \pm 9.5 \times 10^3\text{m}^3$  of water from 1903 to 2004. Basagic states that these numbers should be viewed only qualitatively as area-volume empirical relations are subject to a lot of uncertainty. Still, these numbers provide useful order-of-magnitude information when compared to both the study attempted here and previous mass balance studies.

Yearly melt data inferred from [Basagic and Fountain \[2011\]](#) is consistent with [Tangborn \[1977\]](#), but masks the variability in water balance found by [Dean \[1974\]](#). If the water balance from [Tangborn \[1977\]](#) is of an approximate magnitude to the 2013-2014 water

balances at nearby Lyell Glacier, then the interquartile ranges found in this study are two orders of magnitude above the glacial melt signal. If instead the melt volume is on the order of variability found by Dean [1974], the interquartile ranges found in this study is only an order of magnitude larger than the melt signal.

#### 4.4 Suggestions For Future Studies

This study examined river discharge, snow pillow, land cover, and temperature data from a variety of sources in an attempt to quantify the external fluxes into hydrologic basins within the study area. The three major external fluxes to the system were runoff, precipitation, and evapotranspiration. Of these, only runoff could be directly measured.

This study chose to use a minimum-maximum evapotranspiration estimate based on Lundquist [2011]. However many empirical evapotranspiration models exist which make use of meteorologic data. Fisher [2005] in particular examines different evapotranspiration models as applied to a Sierra Nevada forest ecosystem and may be useful for future water balance models in the area.

This study also ignored all precipitation that fell as rain along with any snowstorms which occurred after peak winter SWE depth. Although this allowed simplification of data analysis, this assumption may have ignored significant water inputs. Future studies should seek to quantify precipitation inputs not immediately visible within the SWE snowpillow data used. Lundquist [2011] use of MODIS remote sensing data may be better suited to the study region, as the large change in topographic character throughout the Lyell fork of the Tuolumne may introduce inaccuracies in SWE vs. Elevation trends.

Equation 2.4 which was used in this study to estimate glacial sensitivity to environmental conditions provides useful parameters for estimating future melt. Although the precision of this study was not enough to derive a useful melt dependence on mean summer temperature parameter, future studies on these two glaciers should include environmental parameter analysis to assist in melt forecasts.

# Bibliography

- Meier M. F. Peckham S.D. Bahr, D. B. The physical basis of glacier volume-area scaling. *Journal of geophysical research.*, 102(B9):20, 1997. ID: 1430106283133.
- Basagic and Fountain. Quantifying 20th century glacier change in the sierra nevada, california. *AARE: Arctic, Antarctic, and Alpine Research*, 43(3):317–330, 2011. ID: 18474768565135.
- Harper J. Humphrey N. Brown, J. Cirque glacier sensitivity to 21st century warming: Sperry glacier, rocky mountains, usa. *Global and Planetary Change*, 74(2):91–98, 2010. ID: 671834476.
- California Department of Water Resources/Snow Surveys, 2015.
- R. R. Currey. Holocene climatic and glacial history of the central sierra nevada, california. *United States contributions to Quaternary research*, page 123, 1969.
- W. W. Dean. Maclure glacier, california: a contribution to the international hydrological decade. *Western Snow Conference*, (42), 1974.
- S. Lawrence Dingman. *Physical Hydrology*. Waveland Press, Inc., 2002. ISBN 1577665619.
- DeBiase Terry A. Qi Ye Xu Ming Goldstein Allen H. Fisher, Joshua B. Evapotranspiration models compared on a sierra nevada forest ecosystem. *Environmental Modelling & Software*, 20(6), 2005. ID: 4587327447.
- G. Karl Gilbert. Variations of sierra glaciers. *Sierra Club Bulletin*, 5(1):20, 1905. URL <https://archive.org/details/sierraclubbullet5105sier>.
- D. R. Hardy. repeat photographic survey of lyell, maclure, dana, and conness glaciers, 1987.
- Elder Kelly Kattelman, Richard. Hydrologic characteristics and water balance of an alpine basin in the sierra nevada. *WRCR Water Resources Research*, 27(7):1553–1562, 1991. ID: 28975156391279.

- Purkey D Young C Kiparsky M, Joyce B. Potential impacts of climate warming on water supply reliability in the tuolumne and merced river basins, california. *PloS one*, 9(1), 2014. ID: 19415535183111.
- Kolmogorov-Smirnov. The kolmogorov-smirnov statistical test. <http://mathworld.wolfram.com/Kolmogorov-SmirnovTest.html>.
- Joseph LeConte. *Ramblings through the High Sierra*. 1900. ID: 18578372.
- Adi Lopez. Mountains of light. Watercolor, 2015.
- D. Jessica; Loheide P. Steven Lundquist. How evaporative water losses vary between wet and dry water years as a function of elevation in the sierra nevada, california, and critical factors for modeling. *Water Resources Research*, 47(1-4):17–26, 2011. doi: 10.1029/2010WR010050.
- Dettinger Michael D. Cayan Daniel R. Lundquist, Jessica D. Snow-fed streamflow timing at different basin scales: Case study of the tuolumne river above hetch hetchy, yosemite, california. *WRCR Water Resources Research*, 41(7), 2005. ID: 28975156486134.
- John Muir. On actual glaciers of california. *American Journal of Science and Arts, Third Series 5*, pages 69–70, 71, 1871.
- John Muir. The yosemite, 2012. ID: 831117567.
- National Park Service. <http://www.nps.gov/yose/learn/nature/vegetation-map.htm>, 1997.
- Department of the Interior National Park Service. Reports of glacier studies in yosemite national park. Technical report, National Park Service, 1931-1975. URL <http://glaciers.us/downloads>.
- National Park Service, Unpublished Glacier Data. 2014.
- National Park Service, Unpublished Hydrologic Data, 2015.
- W. S. B. Paterson and K. M. Cuffey. *Mass Balance Processes: 1. Overview and Regimes*, page 106. Butterworth-Heinemann/Elsevier, Amsterdam; Boston, 2010a. ID: 698912711.
- W. S. B. Paterson and K. M. Cuffey. *Mass Balance Processes: 1. Overview and Regimes*, page 129. Butterworth-Heinemann/Elsevier, Amsterdam; Boston, 2010b. ID: 698912711.

- Brown C. S. Post Austin. Geological Survey (U.S.) Raub, William. Inventory of glaciers in the sierra nevada, california, 2006. ID: 150863427.
- Bales Roger C. Painter Thomas H. Dozier Jeff Rice, Robert. Snow water equivalent along elevation gradients in the merced and tuolumne river basins of the sierra nevada. *WRCR Water Resources Research*, 47(8), 2011. ID: 28975155399860.
- Israel C. Russell. *Existing glaciers of the United States*,. Govt. Print. Off., Washington, 1885. ID: 2046163.
- Solinst Instrument Manuals. Solinst levellogger and instrument manuals, levellogger gold and barologger edge. <http://www.solinst.com/products/dataloggers-and-telemetry/>, 2015.
- Greg Stock. Personal communication, 2015.
- Krimmel Robert M. Mayo L. R. Scully David R. Geological Survey (U.S.) Tangborn, Wendell V. Combined ice and water balances of maclure glacier, california, south cascade glacier, washington, and wolverine and gulkana glaciers, alaska, 1967 hydrologic year, 1977. ID: 896810515.
- Western Regional Climate Center. Precipitation trends for 2011. <http://www.wrcc.dri.edu/articles/19/>.
- Wolfram Alpha. <http://www.wolframapha.com>, 2015.